Public

Report

Document ID	Version	Status	Reg no	Page
1403930	1.0	Approved		1 (53)
Author Jan Hernelind/5T Engineering AB			Date 2013-12-16	
Reviewed by Sabina Hammarberg (QA)			Reviewed date 2014-01-20	
Approved by Jan Sarnet			Approved date 2014-01-21	

Shearing of copper canister at top and base

Background

The aim is to investigate the consequences of the copper shell integrity when shearing occurs close to the lid or close to the base of the copper canister for spent fuel. The geometry is based on the BWR-design.

A simplified elasto-plastic (von Mises) model used for most of the "Earthquake induced rock shear through a deposition hole when creep is considered – first model. SKB R-06-87" (Hernelind 2006) - the material model for the short duration analysis is based on a simplified elastic-plastic material model, using data from the creep model assuming a strain rate of 0.005/second which is considered as conservative.

The flow curve data has been calculated from Sandström et al. (2009). The model is named Global model in this report.

Abstract

This report aim to investigate the copper shell integrity at unfavorable horizontal shearing. Therefore shearing has been performed at the insert lid and at the insert base assuming stiff buffer (bentonite with density 2050 kg/m^3) and with the statistically highest value for yield and ultimate stress limit for the insert. The horizontal shearing has been performed with 1 m/sec to first 5 cm and then followed by further 5 cm (totally 10 cm shearing).
The results show similar maximum level for strains in the copper shell regardless of shearing at the insert lid or at the insert base but generally the strain level is much higher when shearing at the insert lid. The maximum plastic strain at 10 cm shearing is about 30 % but does not imply that the integrity is lost.

Sammanfattning

Rapporten avser att utreda kopparskalets integritet vid ogynnsam horisontell skjuvning. Därför har skjuvning vid insatsens lock och bas studerats med antagande av styv buffert (bentonit med densiteten 2050 kg/m^3) samt med de statistiskt högsta värdena för sträck- och brottgräns för insatsen. Den horisontella skjuvningen har utförts med hastighen 1 m/s till först 5 cm och därefter med ytterligare 5 cm (totalt 10 cm).

Resultaten visar snarlika maximala töjningsnivåer för kopparskalet när skjuvning sker vid insatsen topp eller vid insatsens bas men kopparskalet har generellt betydligt högre töjningsnivåer vid skjuvning vid insatsens topp . Maximala plastiska töjningar vid skjuvning med 10 cm är ca 30 % men medför inte att integriteten går förlorad.

Svensk Kärnbränslehantering AB
Swedish Nuclear Fuel and Waste Management Co
PO Box 925, SE-572 29 Oskarshamn
Visiting address Gröndalsgatan 15
Phone +46-491-76 79 00 Fax +46-491-76 79 30
www.skb.se
556175-2014 Seat Stockholm

Contents

1 Introduction

The copper corrosion barrier should remain intact after a 5 cm shear movement at a velocity of 1 m/s for buffer material properties of a 2,050 kg/m^3 Ca-bentonite, for all locations and angles of the shearing fracture in the deposition hole, and for temperatures down to 0°C. The insert should maintain its pressure-bearing properties to isostatic loads. The most severe shearing positions for the copper shell are close to the lid and at the base, see "Global simulation of copper canister – final deposition" (SKBdoc 1339902).

The copper shell is studied more carefully and especially close to the shearing planes (base and top).

1.1 Context for this report

One important function of the buffer material in a deposition hole in a repository for nuclear waste disposal is to reduce the damage of rock movements on the canister. The worst case of rock movements is a very fast shear that takes place along a fracture and occurs as a result of an earthquake.

The consequences of such rock shear have been investigated earlier, both by laboratory tests (Börgesson et al. 2004), laboratory simulations in the scale 1:10 (Börgesson et al. 1995, 2004), (Bögesson and Hernelind,2010) and finite element modelling (Hernelind 2006, 2010).

Those investigations were focussed on a base case with a horizontal shear plane and Na-bentonite as buffer material.

A sequence of analyses has previously been performed for earthquake induced rock shear. The outcome of these analyses is described by Börgesson and Hernelind (2006).

A final deterministic sequence of analyses have been summarized in Hernelind (2010) where the buffer material properties are based on Ca-bentonite instead of Na-bentonite.

Also copper shell, insert (iron) and steel lid (steel) material properties were based on the most recent experimental results.

This report summarizes the results for shear plane position either close to the base or close to the top and especially the integrity of the copper shell is studied.

2 Simulation strategy for the rock shear analysis

The performed shearing simulations (top and base) are both based on the same geometry and consists of a copper shell, canister (nodular cast iron), cassettes (steel) and insert lid (steel) surrounded by the buffer (bentonite).

3 Geometry definitions and meshes

3.1 General

The geometry used in the analysis of the impact of earthquake induced rock shear consists of the insert (made of nodular cast iron), the insert lid (made of steel) and the copper shell surrounded by buffer material (bentonite). The geometry is based on CAD-geometries received from SKB, "Ritningsförteckning för kapselkomponenter" (SKBdoc 1203875) and should therefore correspond to the current design.

Due to symmetry only one half has been modelled. The mesh is then generated by 3-dimensional solid elements, mainly 8-noded hexahedral (most of them using full integration technique) and a few 6-noded wedge elements.

The model size is defined by about 126,000 elements and 160,000 nodes (total number of variables about 650,000).

The buffer has been partitioned at two different positions defining the rock shear perpendicular to the axis of the canister at the top of the insert lid and at the base, Fig 3-1. Fig 3-2 shows details of the mesh.

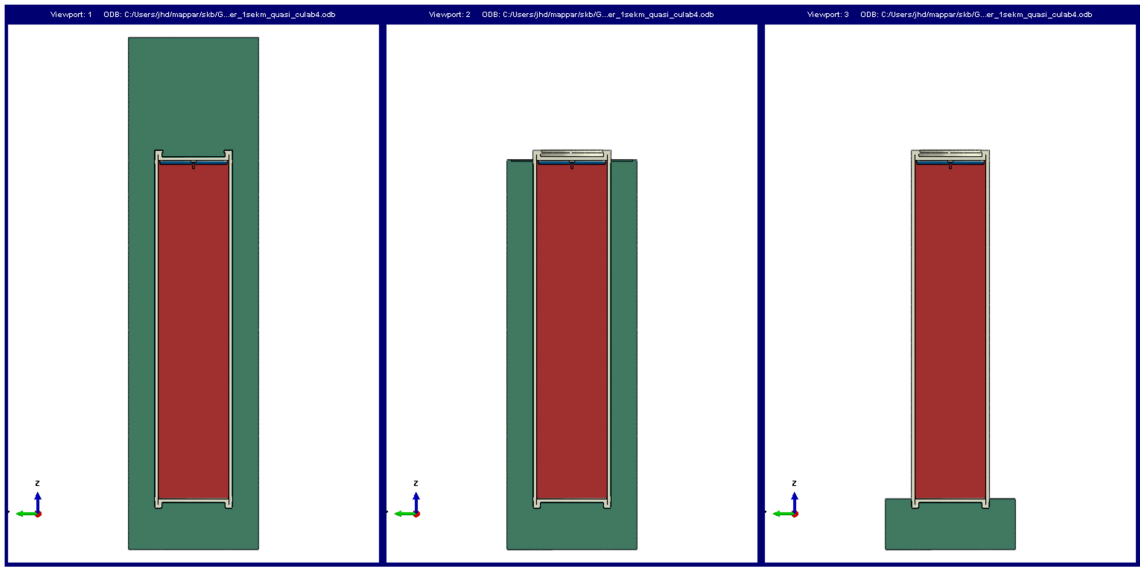

Figure 3-1. *From left to right plot of geometry for rock shear perpendicular to axis of canister, shearing plane at the insert lid and shearing plane at the base.*

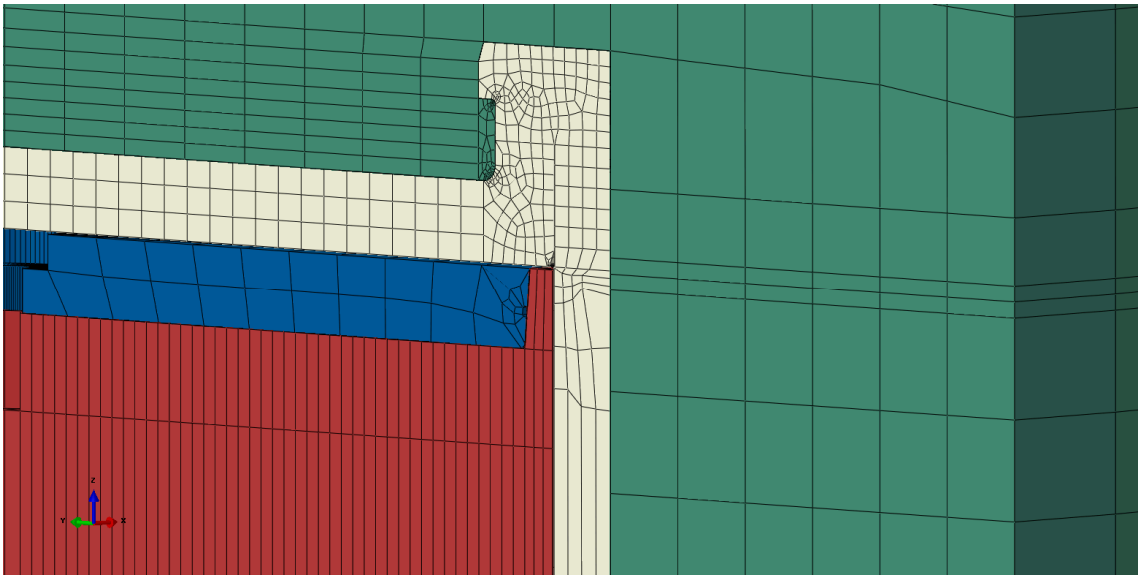

Figure 3-2. *Detail of upper corner showing bentonite (green), copper shell (white), insert lid (blue) and insert (red).*

3.2 Geometry of parts

3.2.1 Deposition hole

The model of the deposition hole has a diameter of 1.75 m and a length of 6.9 m. The canister is placed about 0.5 m above the bottom and about 1.5 m below the top of the deposition hole. Buffer material (bentonite) surrounds the canister and will fill out the deposition hole. The rock shear is then simulated by prescribing boundary conditions at the buffer envelope.

3.2.2 Insert

The insert is made of nodular cast iron and has been simplified regarding the square tubes which are assumed to be tied to the nodular cast iron insert and thus these contribute as added material to the insert. This simplification will probably overestimate stresses and strains in this region.

The insert is modeled as a homogeneous part with 3D solids, see Figure 3-3.

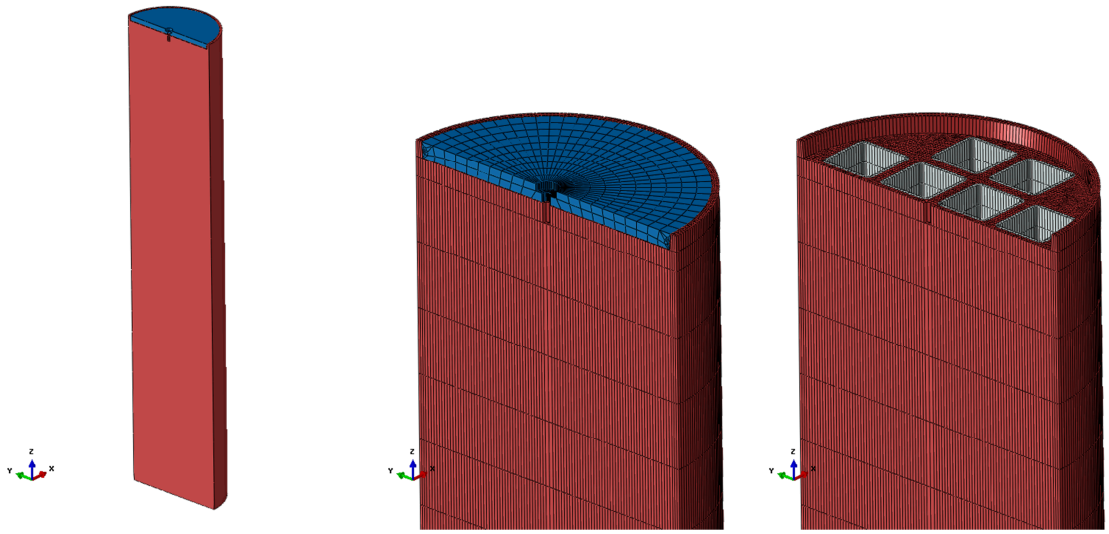

Figure 3-3*. Insert BWR geometry (left), mesh with lid (mid) and without lid (right).*

3.2.3 Insert lid

The insert lid is made of steel and is modelled with 3D solids, see Figure 3-4.

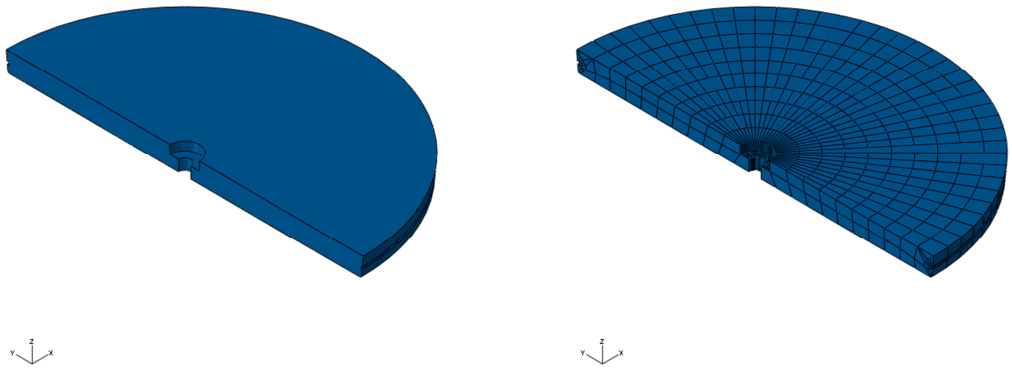

Figure 3-4. *Insert lid geometry (left) and mesh (right).*

3.2.4 Copper shell

The copper shell surrounds the insert and interacts with the buffer and the insert. The canister has been modelled rather accurately in order to catch “hot spots” where large strains are expected, e.g. the fillets at the base and top (the copper lid). The lid is welded to the flange and lid and canister will act as one part, see Figure 3-5.

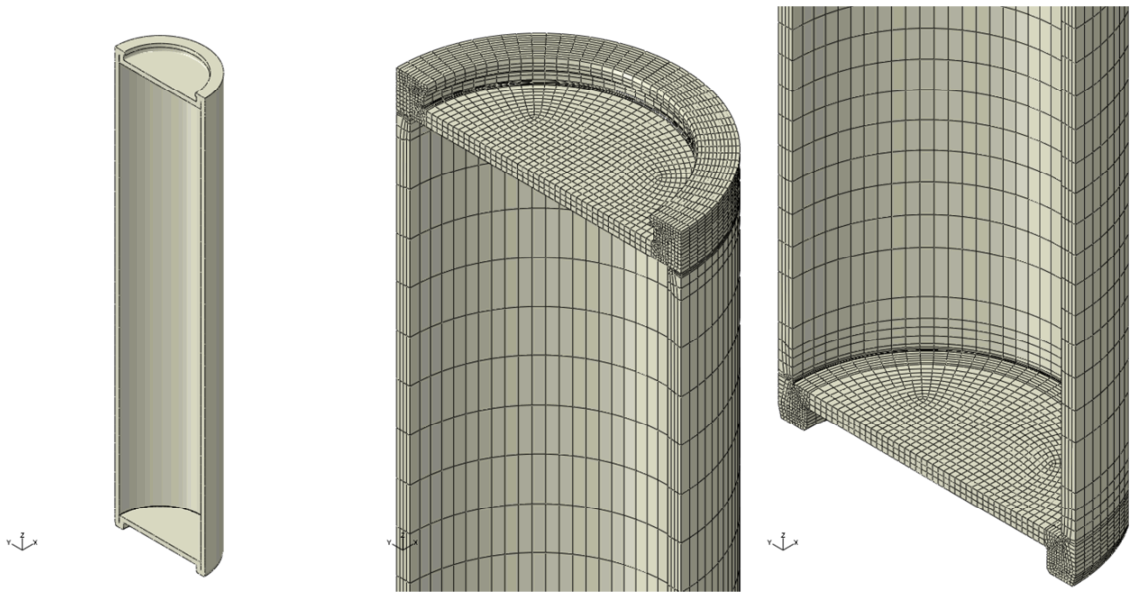

Figure 3-5*. Copper shell geometry (left), mesh top (mid) and mesh base (right).*

4 Material models

The finite element code ABAQUS was used for the calculations. The materials have been modelled as elastic-plastic with stress-strain properties that correspond to each material and the applied shear load induced strain rate, when applicable.

4.1 Nodular cast iron (used by the insert)

The material model for the insert is based on a von Mises' material model with elastic behaviour defined by Young's modulus and the Poisson's ratio and the plastic behaviour defined through yield surface (true stress) versus plastic strain (defined as logarithmic strain), see Table 4-1 and Figure 4-1. The numbers in Table 4-1 are derived from the mean value stress/strain curve in section 3.2 and high yield/ultimate stress values in 4.4 (SKBdoc 1336557). The mean value curve is then scaled for the intermediate values assuming that the equivalent plastic strain is valid. The last row is arbitrarily defined at 10 MPa and is used only as an indication of failure.

The experiments were performed at 20 ^{o}C (room temperature).

Table 4-1. Stress-strain definition for insert at tension (but used also in compression).

Plastic Strain (%)	True stress (MPa) at low strain rate	
	high-high	Strain rate factor at strain rate=0.5
0	314.2	1.19
1.79	355.9	1.13
3.70	393.9	1.10
5.59	424.9	1.10
7.45	447.0	1.09
9.27	463.7	1.09
11.83	480.8	1.08
12.99	10.0	1.08

The strain rate dependency is defined by assuming that the yield surface is proportional to the strain rate factor (at the strain rate 0.5 1/s the factor 1.08 has been chosen and at strain rate 0 1/s the factor is 1.0).The instantaneous strain rate factor is then linearly interpolated between 1 and 1.08 using the instantaneous strain rate.

Furthermore, Young's modulus E = 166 GPa and Poisson's ratio $\nu = 0.32$.

Material properties have been derived for yield and ultimate stress. The following values are derived for the yield stress (technical stress/true stress) (SKBdoc 1336557):

- High yield stress 313.6/314.2 MPa

Also the ultimate stress is derived:

- High ultimate stress 418.3/480.8 MPa

For the analyses of shearing placed at the steel lid and at the base material properties for "high yield stress" and "high ultimate stress" have been used.

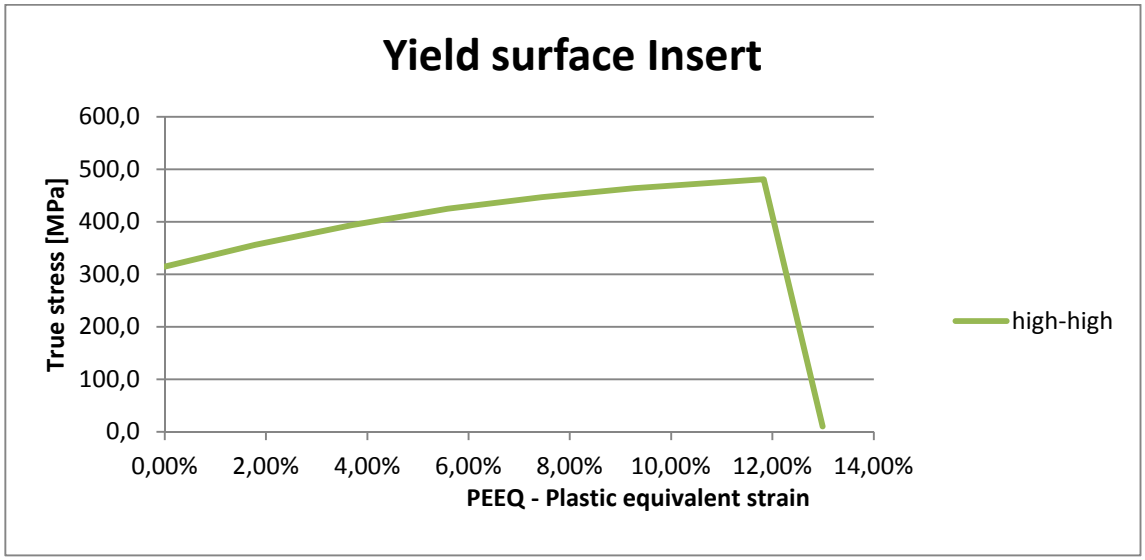

Figure 4-1. *Yield surface [MPa] versus plastic strain [%] for high yield stress and high ultimate stress at low strain rate.*

4.2 Steel (used by the channel tubes in the insert)

The material model for the channel tubes in the insert is based on a von Mises' material model with elastic behaviour defined by Young's modulus and the Poisson's ratio. The plastic behaviour is defined through yield surface (true stress) versus plastic strain (using logarithmic strain).

The steel cassette tubes are manufactured by steel S355J2H, for example Domex 355 MC B. SKB has earlier supplied test data for the yield point of their material, however no stress-strain data to be used in a plastic analysis. The stress-strain curve for Domex 355 MC B (SSABDirect 2008) can be scaled using the yield stress and tensile ultimate strength measured by SKB, Re = 412 MPa (yield stress) and Rm = 511MPa (ultimate stress). With this procedure a simplified stress-strain curve is obtained and described by Table 4-2.

Table 4-2. Stress-strain definition for channel tubes used in the insert.

Strain (%)	Stress (MPa)	Log Strain (%)	True Stress (MPa)
0	0	0	0
0.196	412	0.196	412
15	509	14.3	587
20	511	18.5	613

Furthermore, Young's modulus E = 210 GPa and Poisson's ratio ν = 0.3.

The data with lowest value from the experiment has been chosen for the yield surface. However, the plasticity definition for the steel channel tubes has very minor influence on the overall results.

4.3 Steel (used by the insert lid)

The material model for the insert lid is based on a von Mises' material model with elastic behaviour defined by Young's modulus and the Poisson's ratio. The plastic behaviour is defined through yield surface (true stress) versus plastic strain (calculated as logarithmic strain).

Manufacturing drawings for the lid specify steel S355J2G3. Strain versus stress for steel Domex 355 MC B with Re = 389 MPa (yield stress) and Rm = 484 MPa (ultimate stress) can be found from SSABDirect (2008). According to SS-EN 10025-2:2004) the material S355 with nominal

thickness 40-63 mm has *Re* = 335 MPa (yield stress) and *Rm* = 470-630 MPa (ultimate stress). Scaling stress-strain curves for Domex 355 by the minimum values given in SS-EN 10025-2 implies the simplified material definition (engineering data) shown in Table 4-3.

Table 4-3. Stress-strain definition for the insert lid.

Strain (%)	Stress (MPa)	Log Strain (%)	True Stress (MPa)
0	0	0	0
0.1595	335	0.1593	335
15	470	13.98	540
20	470	18.2	564

Furthermore, Young's modulus E = 210 GPa and Poisson's ratio ν = 0.3.

The data with lowest value from the experiments (SS-EN 10025-2:2004) has been chosen for the yield surface. However, the plasticity definition for the insert lid has very minor influence on the overall results.

4.4 Bentonite model (used for the buffer)

The bentonite is modelled based on recent experiments, see Börgesson et al. (2010) and adapted to the actual density of the bentonite. The bentonite buffer is modelled using only total stresses that do not include the pore water pressure, the reason being the very fast compression and shear.

The most important properties of the bentonite for the rock shear are the stiffness and the shear strength. These properties vary with bentonite type, density and rate of strain. Ca-bentonite has higher shear strength than Na-bentonite and the shear strength increases with increasing density and strain rate. Since it cannot be excluded that the Na-bentonite MX-80 will be ion-exchanged to Ca-bentonite the properties of Ca-bentonite is used in the modelling. The acceptable density at saturation of the buffer material is 1950 kg/m^3 - 2050 kg/m^3 which is covered by the models below.
The material model is in ABAQUS expressed with the von Mises' stress σ_j that describes the "shear stress" in three dimensions according to Equation 4-1.

$$\sigma_j=(((\sigma_1- \sigma_3)^2 + (\sigma_1- \sigma_2)^2 + (\sigma_2- \sigma_3)^2)/2)^{1/2} \quad (4\text{-}1)$$

where

σ_1, σ_2 and σ_3 are the principal stress components.

The material model defines the relation between the stress and the strain and is partitioned in elastic and plastic parts. For details regarding definition of the shear strength and the influence of density, pressure and rate of shear see Börgesson et al. (1995, 2004).

Rate dependent elastic-plastic stress-strain relation

The elastic-plastic stress strain relations used for the three different densities are derived according to the description above in an identical way as the relations used in all previous calculations.

The bentonite is modelled as linear elastic combined with the von Mises plastic hardening - Table 4-4 shows the elastic constants. The plastic hardening curve is made a function of the strain rate of the material. The reason for the latter relation is that the shear strength of bentonite is rather sensitive to the strain rate. It increases with about 10 % for every 10 times increase in strain rate. Since the rock shear at an earthquake is very fast (1 m/s) the influence is strong and the resulting shear strength will be different at different parts of the buffer. Figure 4-2 shows the material model. The stress-strain relation is plotted at different strain rates.

Table 4-4. Elastic material data for the bentonite buffer Na converted to Ca.

Density/Swelling pressure	Elastic part	
	E (MPa)	ν
Low - 1950/5.3	243	0.49
Mean - 2000/8	307	0.49
High - 2050/12.3	462	0.49

The experiments (Börgeson et al. 2010) show that also Young's modulus E is dependent on strain rate but in the calculations this has been neglected and a representative stiffness has been chosen (sensitivity analyses did show minor changes of the results when varying Young's modulus between maximum and minimum values achieved from the experiments).

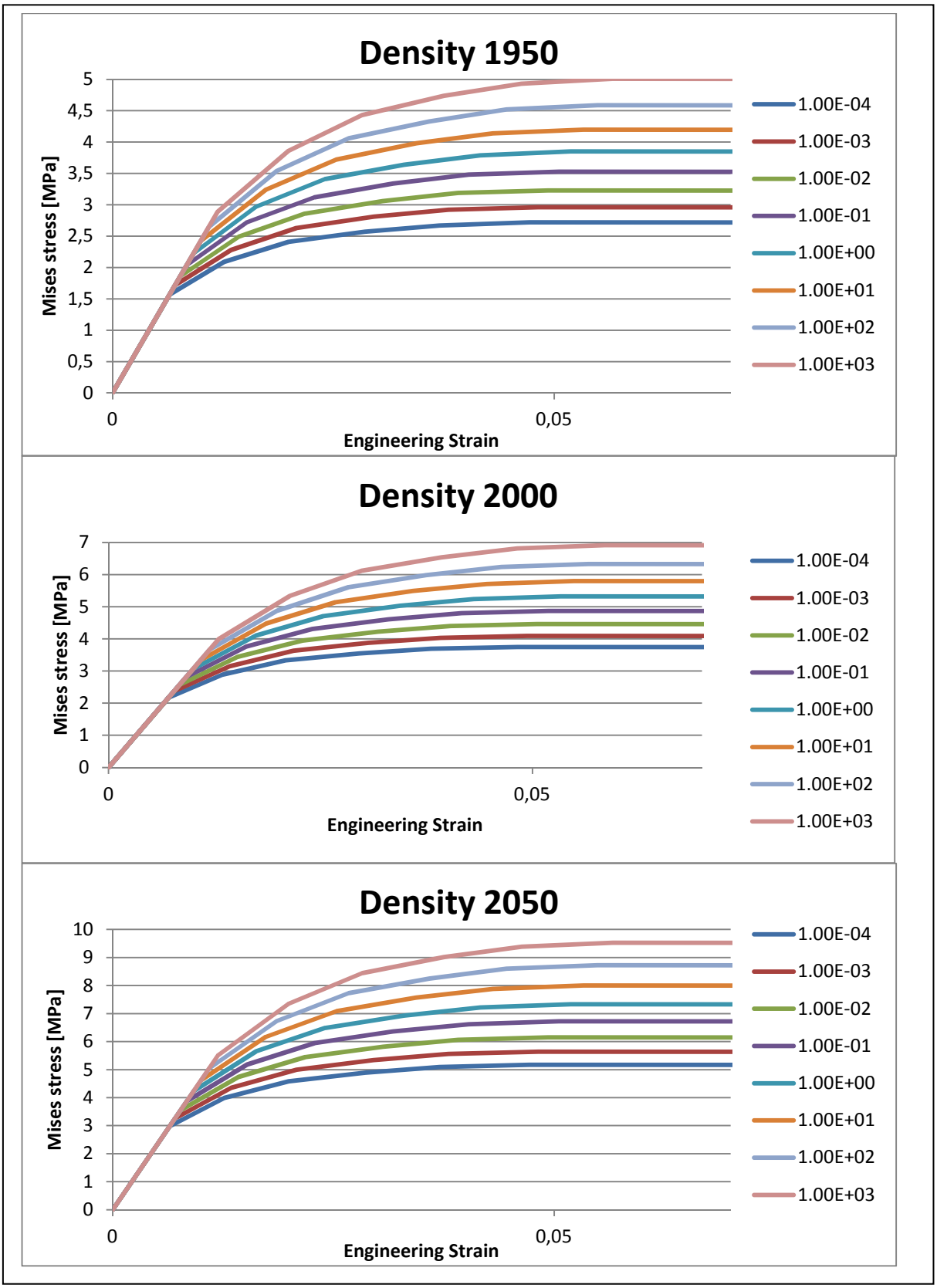

Figure 4-2. *Plot of material definition for the bentonite buffer for different densities and strain rates (Mises stress [MPa] versus engineering strain [1/s]).*

4.5 Copper material model

4.5.1 Kimab material

The material model used for copper for most of the global analyses is described below.
The stress-strain properties of the copper in the copper shell were investigated by the Corrosion and metals research institute Swerea Kimab and the results are then represented by a creep material model developed by Rolf Sandström, see Sandström and Andersson (2008), Jin and Sandström (2008) and Sandström et al. (2009).

The material model for the short duration rock shear analysis is based on a simplified elastic-plastic material model, see Table 4-5, using data from the creep model assuming a strain rate of 0.005/s which is considered as conservative.

The flow curve data has been calculated from Sandström et al. (2009) wherein eq.(17) has been used together with the parameter values defined in the corresponding Table 4-2, (Sandström et al. 2009) as well as $m = 3.06$, $\alpha = 0.19$, $\omega = 14.66$ assuming an average strain rate of 0.005/s.

The maximum strain rate in the copper shell is of order 1/s which implies a stiffer material then using the average strain rate data but implies a conservative estimate of the calculated copper shell strain level.

The copper model data is shown in Figure 4-3.

Table 4-5. Elastic-plastic material data for the copper at strain rate 0.005/s.

Elastic part		Plastic part: von Mises stress σ_j (MPa) at the following plastic strains (ε_p)					
E (MPa)	ν	0	0.10	0.20	0.30	0.40	0.50
$1.2 \cdot 10^5$	0.308	72	178	235	269	288	300

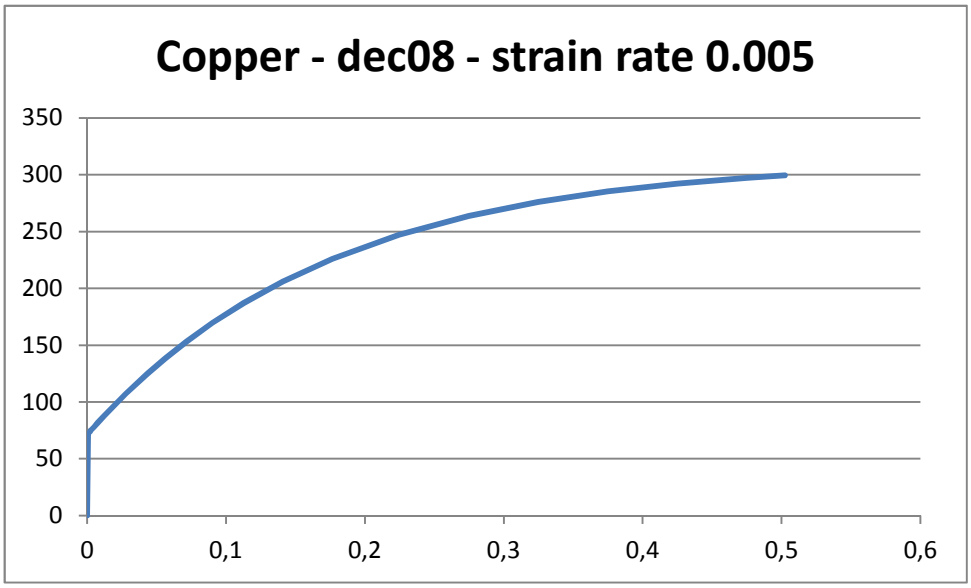

Figure 4-3. *Copper shell material model gives the Mises stress [MPa] as a function of the engineering strain.*

5 Contact definitions

All the boundaries of the buffer, the copper shell, the insert and the insert lid interact through contact surfaces allowing finite sliding. All contact surfaces have friction at sliding with no cohesion and the friction coefficient 0.1, i.e. the friction angle (ϕ) and cohesion (c) are:

$\phi = 5.7^{\circ}$

c=0 kPa

The contact is released when the contact pressure is lost.

A few contact pairs are tied together (tied means that the surfaces are constrained together and will not allow for opening/closing or sliding) in order to improve the numerical convergence rate. This applies at the contact pairs between the insert and insert lid and also at the bottom of insert and copper shell bottom.

The interaction between the buffer and the rock (not modelled) is assumed to be tied through prescribed boundary conditions and will not allow for opening/closing or sliding.

6 Initial conditions

Initial conditions are defined as:

- In the first step initial stresses corresponding to the swelling pressure plus the 5 MPa hydrostatic pressure (the deposition is made about 500 meters below the surface) in the bentonite is applied. However, since the canister deforms when the initial stresses are applied the actual magnitude of the swelling pressure will decrease. For that reason the initial pressure for bentonite with density 2050 kg/m^3 (and measured swelling pressure of 12.3+5 MPa) is given as 40.2 MPa. One observation is that the swelling pressure will vary both in the axial and radial direction which means that it's not possible to have the correct swelling pressure without using elements with pore pressure as a degree of freedom (ABAQUS have those elements but the material model is tuned to total stresses and not effective stresses).

7 Boundary conditions

Symmetry conditions have been specified for the symmetry plane (displacements in the normal direction to the symmetry plane prescribed to zero), see Fig 7-1.

The surrounding rock has been simulated by prescribing the corresponding displacements at the outer surface of the buffer and depends also on type of simulation.

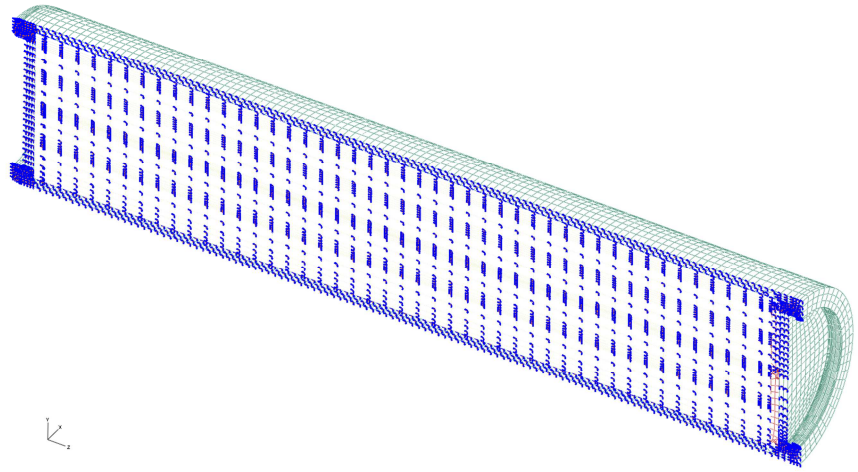

Figure 7-1. *Prescribed symmetry conditions*

8 Calculations

8.1 General

8.1.1 Rock shear calculation cases

The reference case for BWR is based on Na-bentonite converted to Ca-bentonite with density 2050 kg/m^3.

Two cases of rock shear positions have been analyzed.

rock shear perpendicular to the axis of the canister

- at the top of the steel lid
  - n34b_finer_1sekm_quasi - copper: Global model
- at the base of the insert
  - n49b_finer_1sekm_quasi - copper: Global model

8.1.2 Analysis approach

The numerical calculations are performed using the FE-code ABAQUS (ABAQUS 2012) version 6.12 assuming non-linear geometry and material definitions. This means that all non-linearities defined by the input will be considered such as large displacements, large deformations, non-linear interactions (contact) and non-linear materials.

All non-linear contributions will be used when forming the equations to be solved for each equilibrium iteration.

Short term analysis is based on static response but the results will depend on the time used for the simulation since rate-dependent material data is used.

The code will choose suitable time-increments for the loading based on (in most cases) default convergence tolerances.

8.2 Short term analyses

The short term analyses (few seconds) consist of three steps where the shearing is prescribed by boundary conditions. In the first step initial stresses corresponding to the swelling pressure plus the 5 MPa hydrostatic pressure (the deposition is made about 500 meters below the surface) in the bentonite is applied. However, since the canister deforms when the initial stresses are applied the actual magnitude of the swelling pressure will decrease. For that reason the initial pressure for bentonite with density 2050 kg/m^3 (and measured swelling pressure of 12.3+5 MPa) is given as 40.2 MPa. One observation is that the swelling pressure will vary both in the axial and radial direction which means that it's not possible to have the correct swelling pressure without using elements with pore pressure as a degree of freedom (ABAQUS have those elements but the material model is tuned to total stresses and not effective stresses).

In the second step 5 cm is used for the shearing magnitude and finally the third step defines additional 5 cm shearing. The results at 10 cm shearing are used for comparison.

The shearing rate 1 m/sec has been used.

The results for BWR are shown in Appendix 1-2 for density 2050 kg/m^3.

9 Results for rock shear

For each analysis a large amount of results are available and to have an indication only a few values are reported. For the short term rock shear analyses the peak values for Mises' stress, axial stress and plastic strain (PEEQ) are compared when shearing at the lid and at the bottom.

Buffer

The highest value for PEEQ, about 29.4 occurs when shearing at the base, see Figs 9-1 and 9-2.

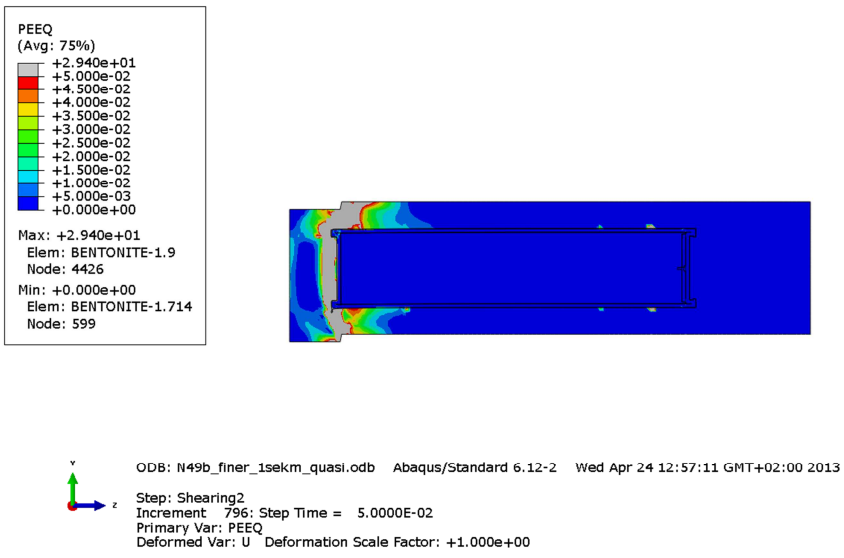

Figure 9-1. *Plot of plastic equivalent strain (PEEQ) when shearing at the base of the insert (10 cm).*

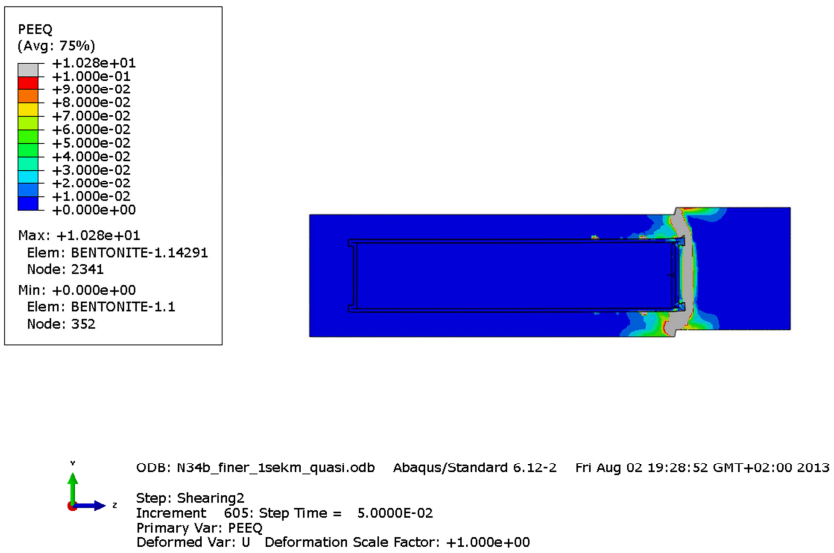

Figure 9-2. *Plot of plastic equivalent strain (PEEQ) when shearing at the lid (10 cm).*

Cast iron insert

The highest value for Mises stress, 426 MPa, occurs for case N34b_finer_1sekm_quasi (with shearing position at the lid) with 10 cm shearing. See Figs 9-3 and 9-4.

No plastic strains occurred for the cast iron insert, see Figs 9-5 and 9-6.

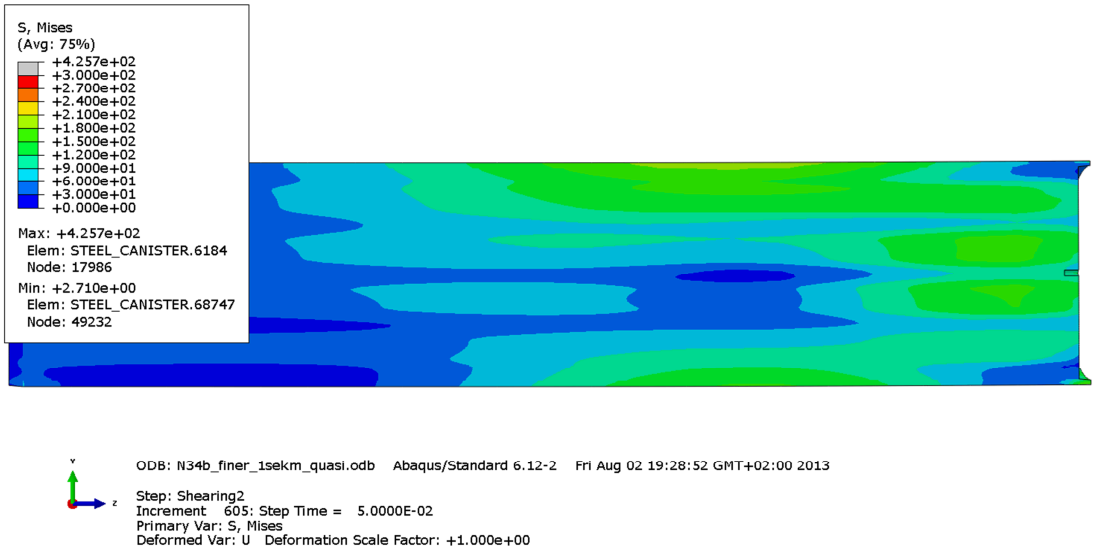

Figure 9-3. *Plot of maximum Mises stress [MPa] in the cast iron insert at 10 cm shearing at the lid.*

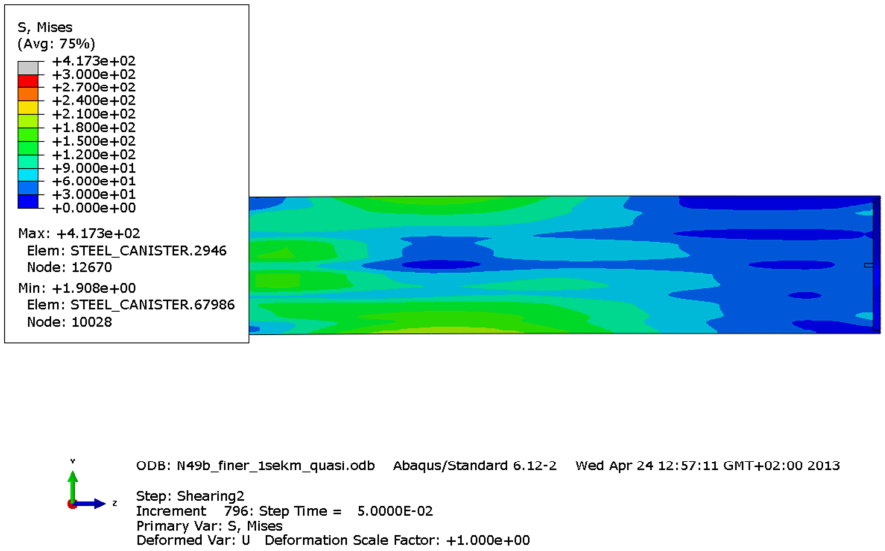

Figure 9-4. *Plot of maximum Mises stress [MPa] in the cast iron insert with 10 cm shearing at the base of the insert).*

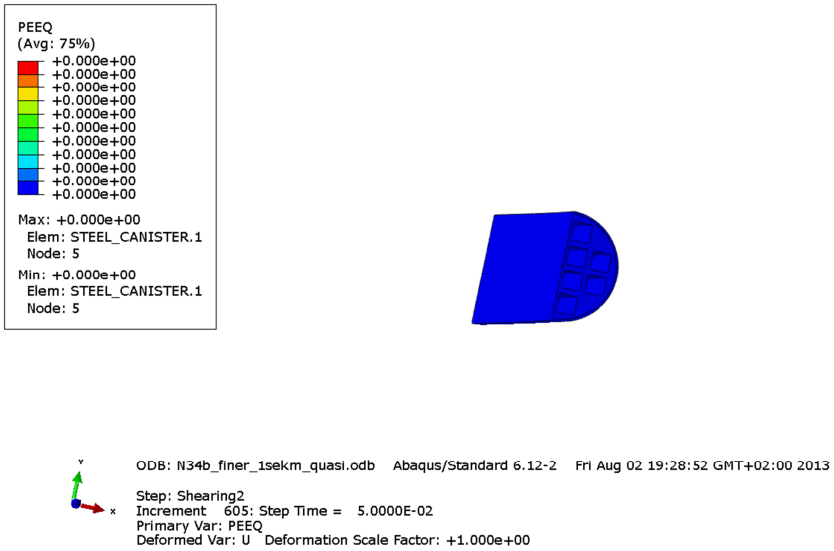

Figure 9-5. *Plot of PEEQ in the cast iron insert with 10 cm shearing at the lid.*

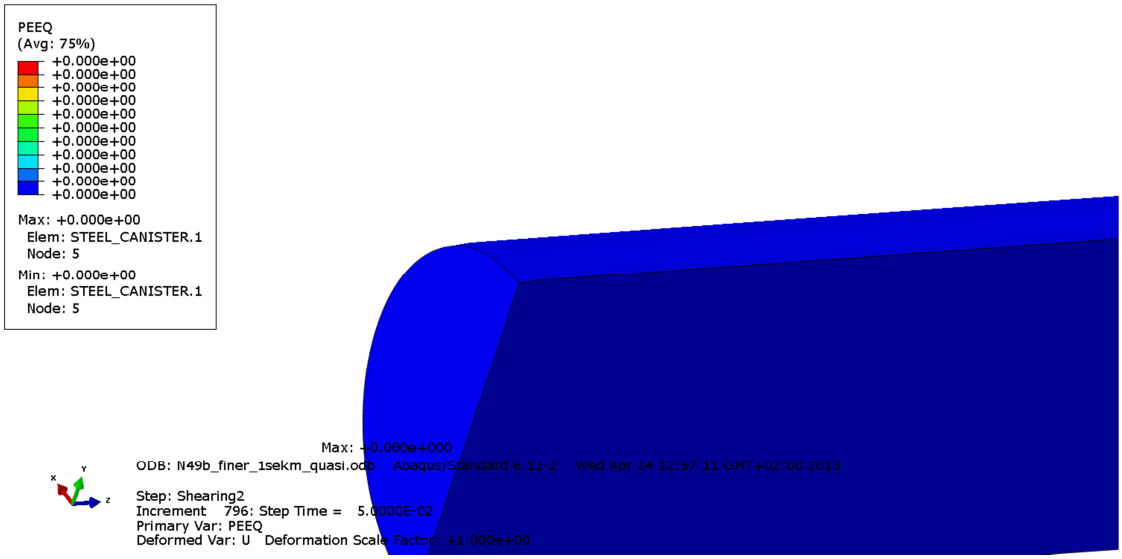

Figure 9-6. *Plot of PEEQ in the cast iron insert with 10 cm shearing at the base of the insert.*

Steel channels

The highest value for the Mises stress, 426 MPa, occurs for case N34b_finer_1sekm_quasi (shearing at the lid), see Fig 9-7 with pure elastic response.

The axial stress, S33, reach about 172 MPa for the same case.

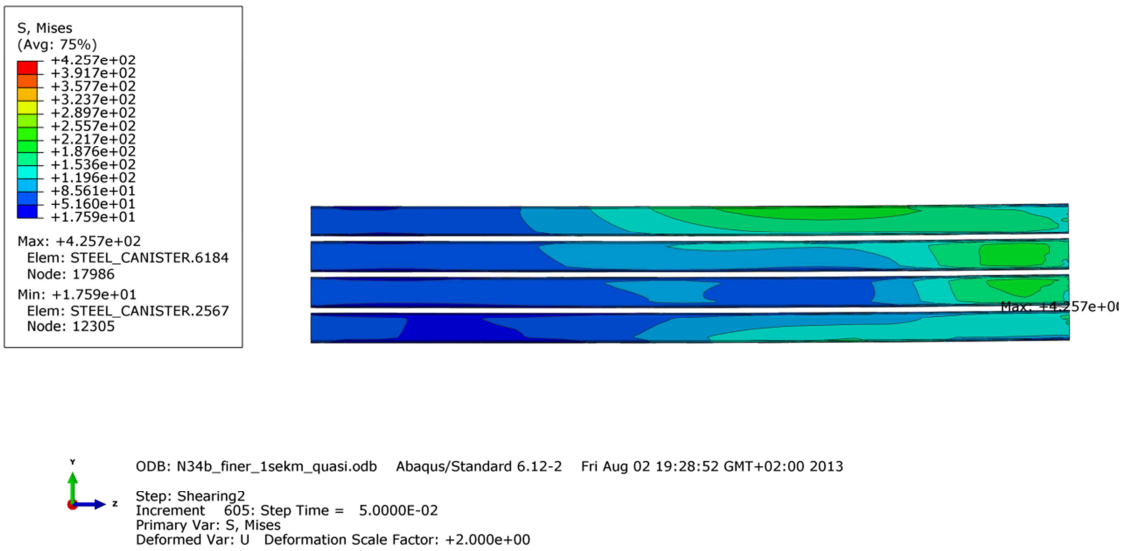

Figure 9-7. *Plot of Mises stress [MPa] in the cast iron insert with 10 cm shearing at base of the insert.*

Output regions copper shell

The peak values for Mises stress and plastic strain occur at a few “hot spots” and therefore the results for the copper shell are reported for nine regions (in the cylindrical part, in areas containing the welds (top and bottom), in areas containing geometric discontinuity (top and base), the fillet regions (top and base) and finally the remaining regions (top and base), see Fig 9-8.

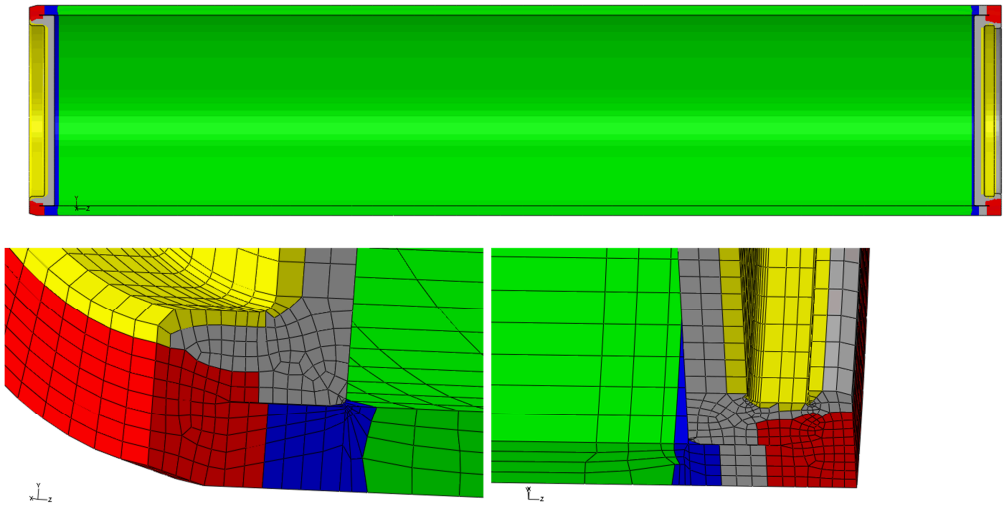

Figure 9-8. *Output regions for copper shell. Region 1 - mid canister (green). Region 2 – top weld (red, lower right). Region 3 – base weld (red, lower left). Region 4 – top discontinuous geometry (blue, lower right). Region 5 – base discontinuous geometry (blue, lower left). Region 6 – top fillet (yellow, lower right). Region 7 – base fillet (yellow, lower left). Region 8 – top reminding (grey, lower right). Region 9 – base reminding (grey, lower left)*

Copper shell

The maximum Mises stress, 256 MPa occurs for case N49b_finer_1sekm_quasi with 10 cm shearing at the base of the insert, see Fig 9-9 – 9-12.

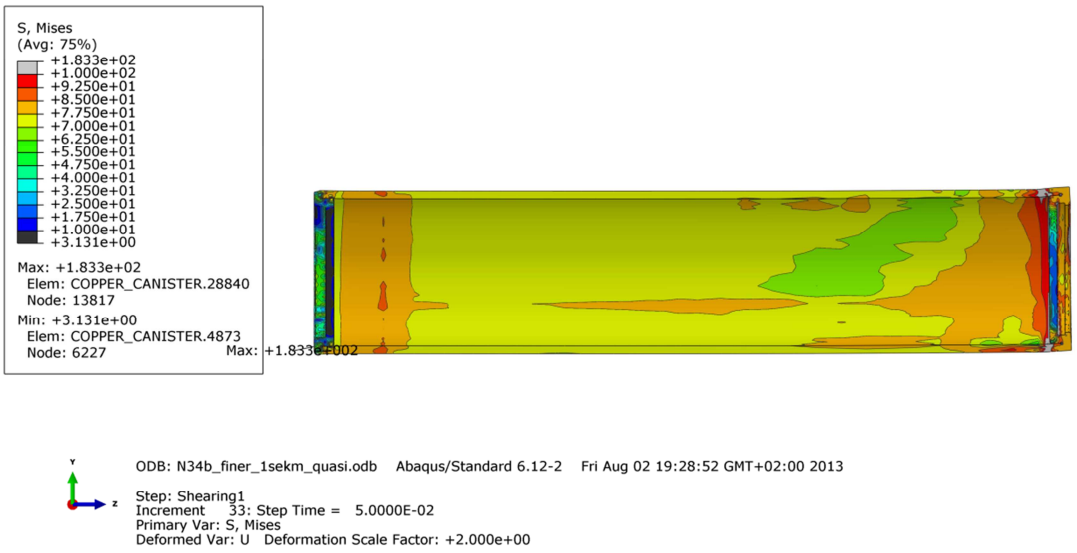

Figure 9-9. *Plot of Mises stress [MPa] in the copper shell with 5 cm shearing at the lid.*

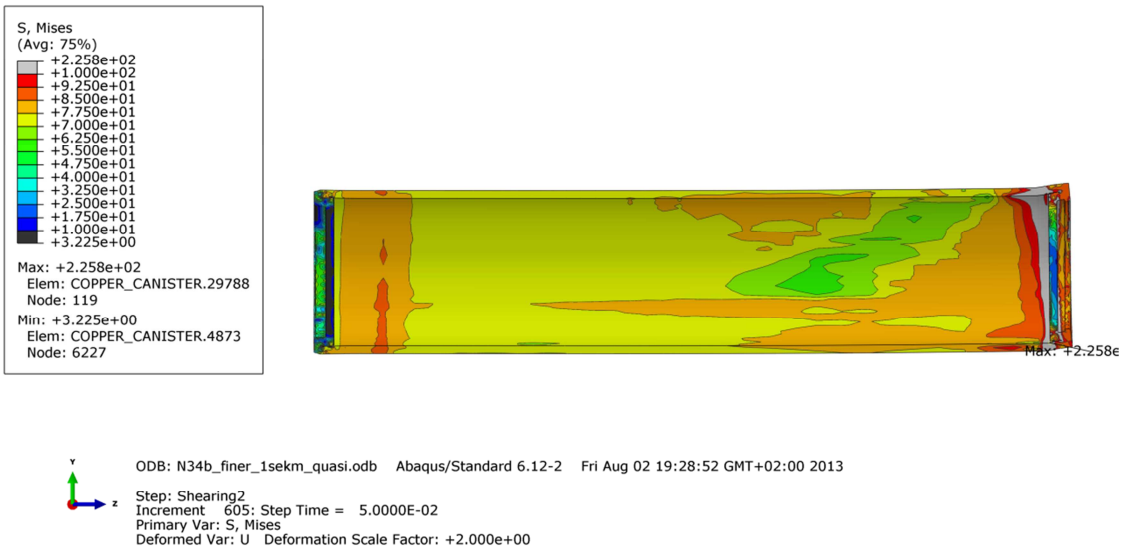

Figure 9-10. *Plot of Mises stress [MPa] in the copper shell with 10 cm shearing at the lid.*

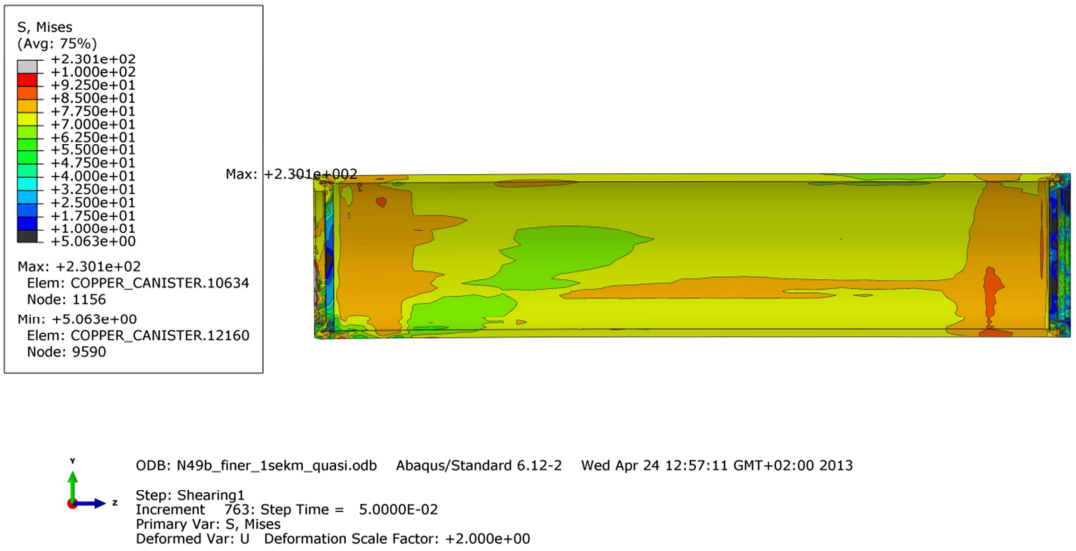

Figure 9-11. *Plot of Mises stress [MPa] in the copper shell with 5 cm shearing at the base of the insert.*

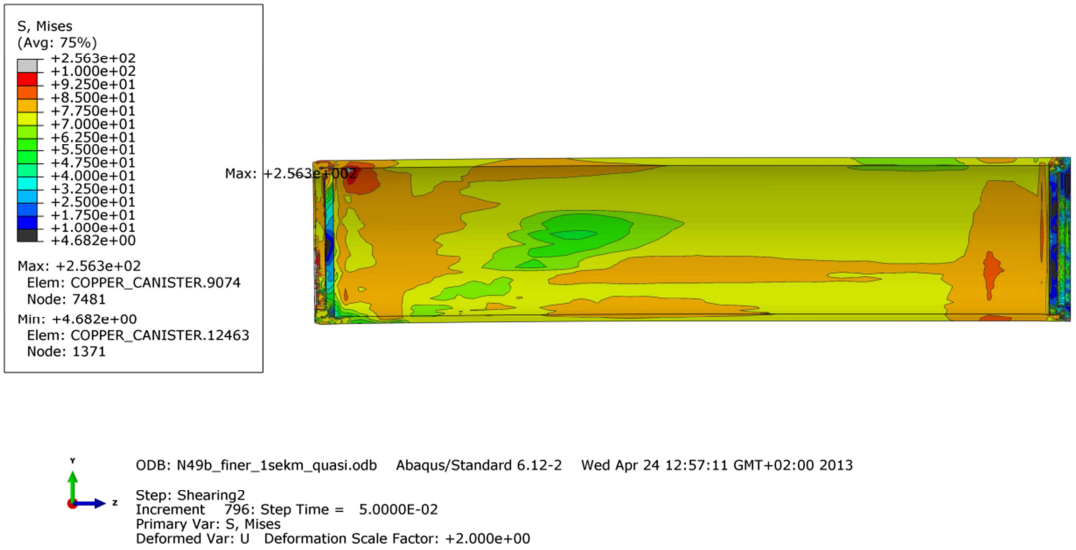

Figure 9-12. *Plot of Mises stress [MPa] in the copper shell with 10 cm shearing at the base of the insert.*

The highest value for PEEQ in the copper shell, 32% (Fig. 9-19), occurs for case N49b_finer_1sekm_quasi with 10 cm shearing at the base of the insert. However, the largest values are at the base where the geometry is discontinuous and these are regions where maximum values strongly depend on the mesh density. Besides the singular regions the highest value occurs at the top and base fillets, see Figs 9-13 – 9-20.

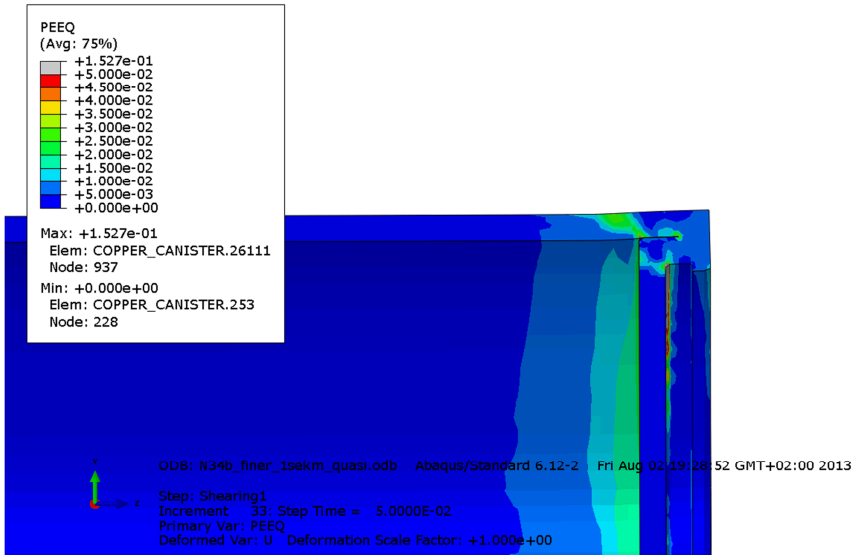

Figure 9-13. *Plot of PEEQ in the copper shell with 5 cm shearing at the lid (top right corner).*

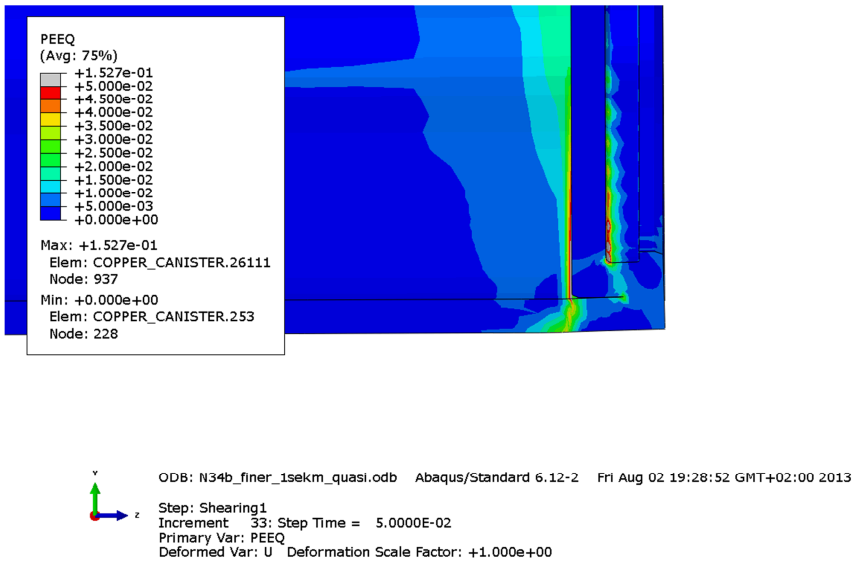

Figure 9-14. *Plot of PEEQ in the copper shell with 5 cm shearing at the lid (bottom right corner).*

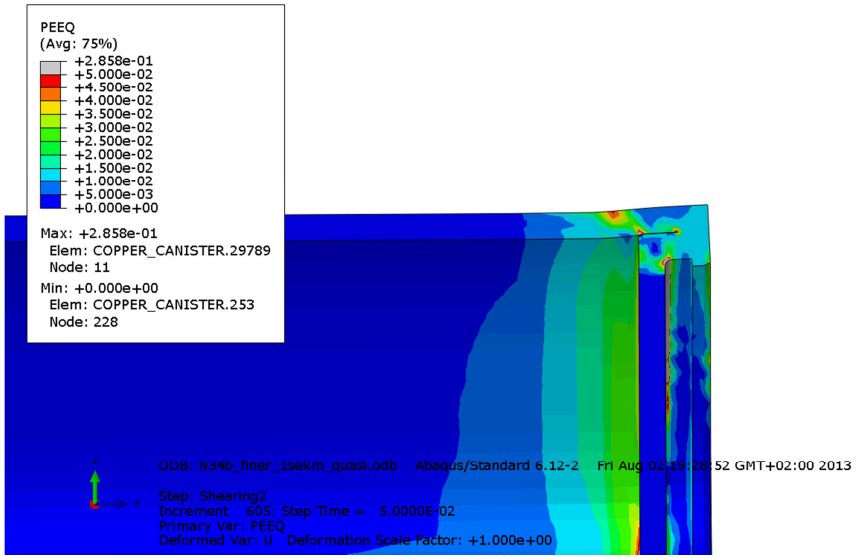

Figure 9-15. *Plot of PEEQ in the copper shell with 10 cm shearing at the lid (top right corner).*

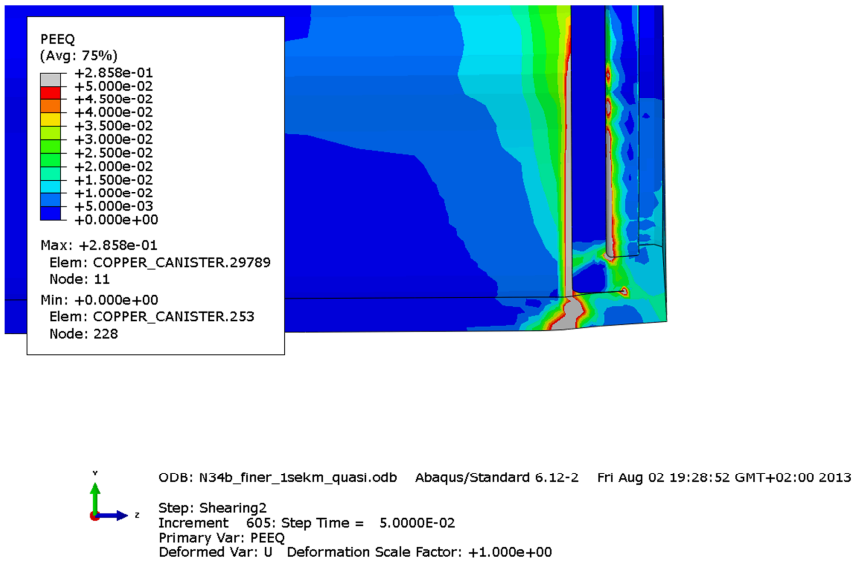

Figure 9-16. *Plot of PEEQ in the copper shell with 10 cm shearing at the lid (bottom right corner).*

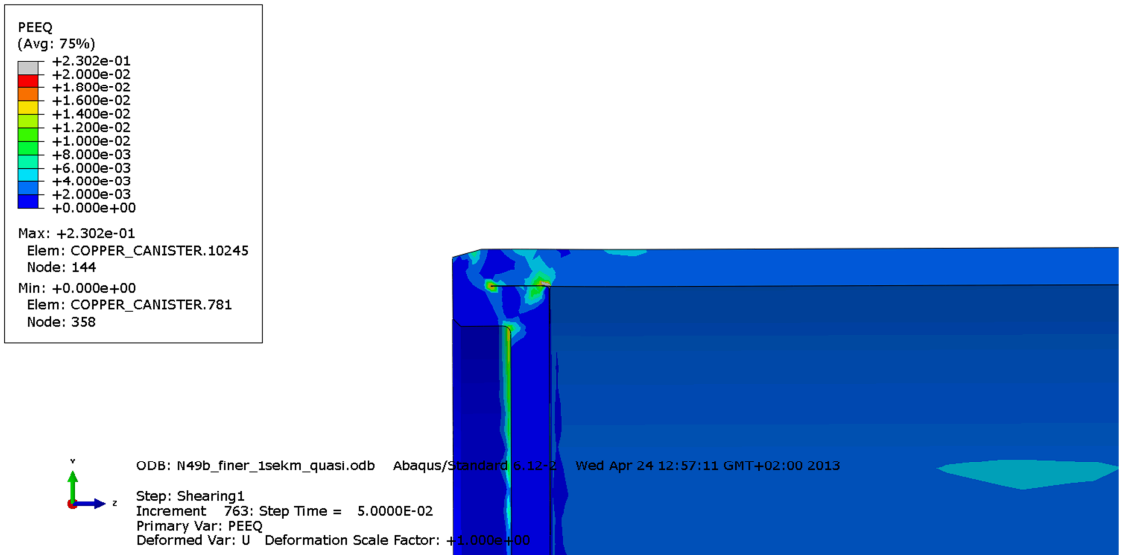

Figure 9-17. *Plot of PEEQ in the copper shell with 5 cm shearing at the base of the insert (top left corner).*

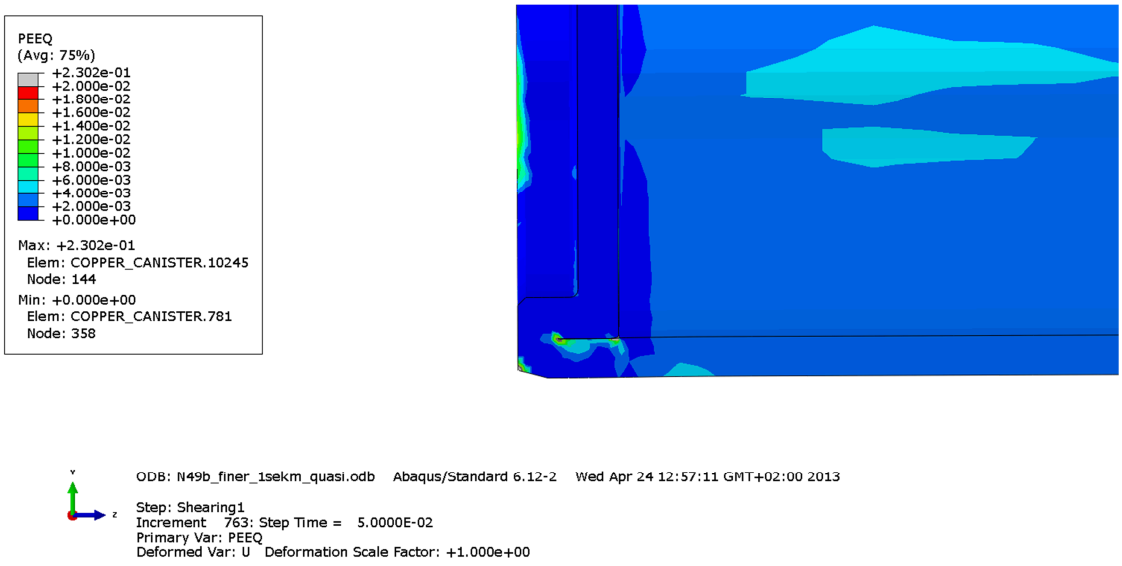

Figure 9-18. *Plot of PEEQ in the copper shell with 5 cm shearing at the base of the insert (bottom left corner).*

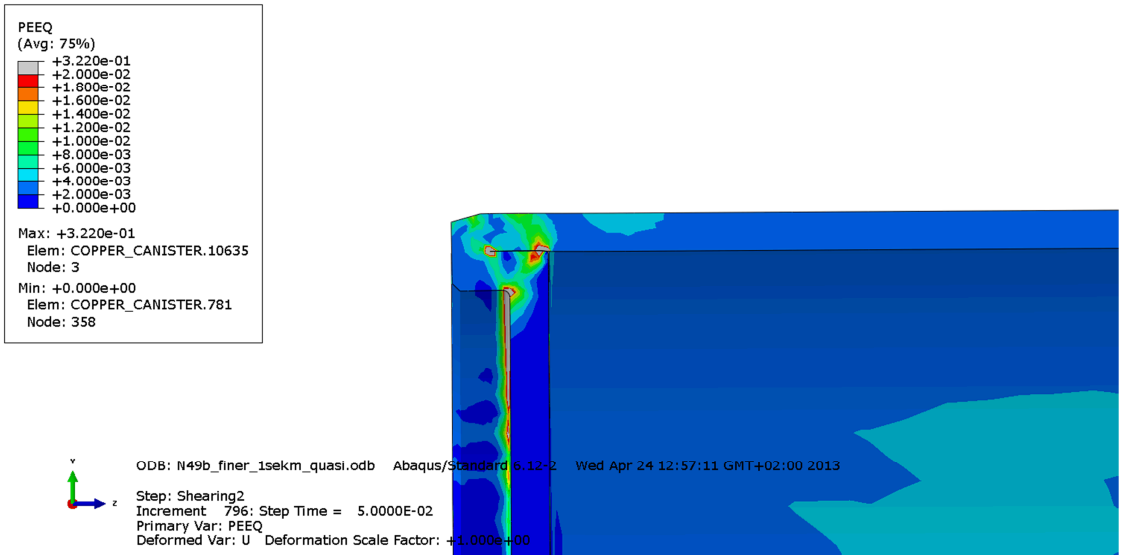

Figure 9-19. *Plot of PEEQ in the copper shell with 10 cm shearing at the base of the insert (top left corner).*

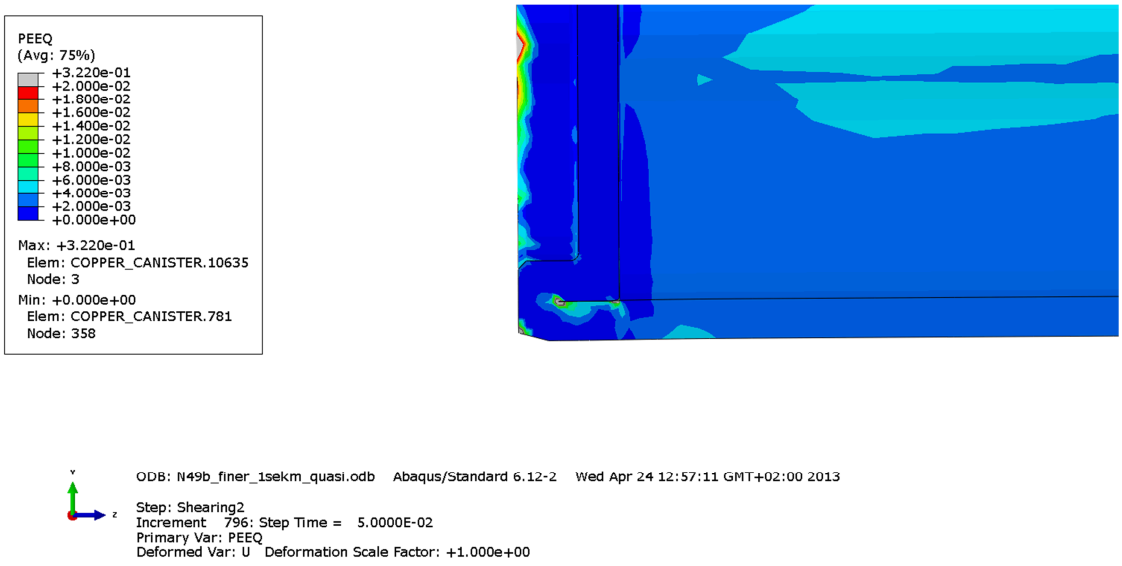

Figure 9-20. *Plot of PEEQ in the copper shell with 9 cm shearing at the base of the insert (bottom left corner).*

Figs 9-21 – 9-24 show plots of deformed geometry with and without the buffer. The deformation has been magnified. Fig 9-25 shows displaced geometry with contours of PEEQ (plastic equivalent strain) and clearly shows that even though the maximum PEEQ is similar for shearing at the insert top and insert base the overall strain level is much higher when shearing at the insert lid.

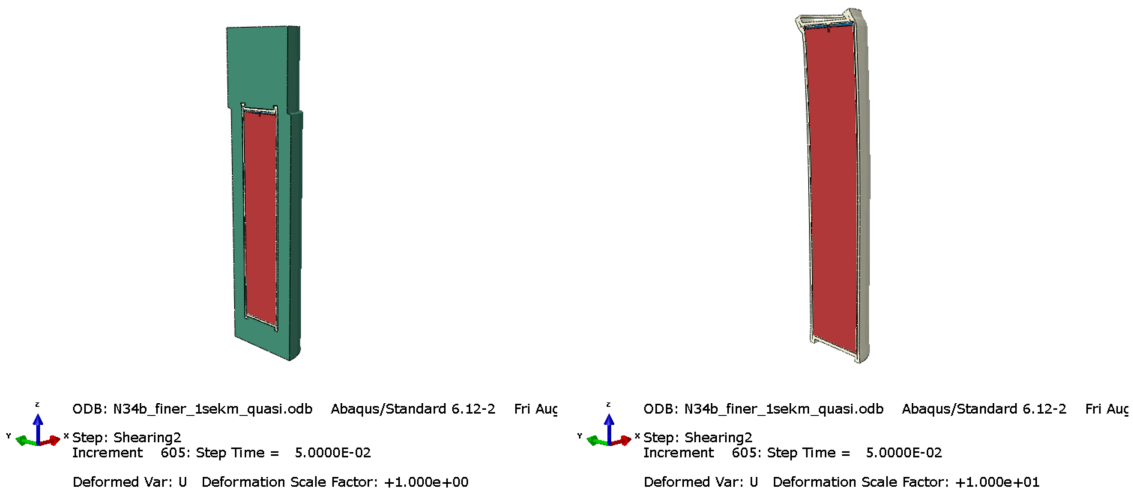

Figure 9-21. *Displaced geometry with scale factor 1 (left) and with scale factor 10 (right) when shearing at the insert lid with shearing magnitude 10 cm.*

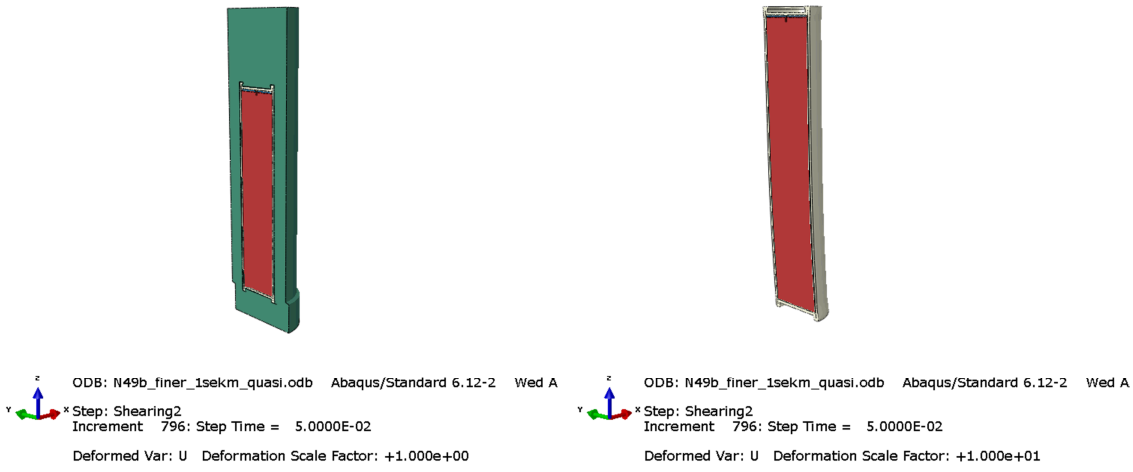

Figure 9-22. *Displaced geometry with scale factor 1 (left) and with scale factor 10 (right) when shearing at the insert base with shearing magnitude 10 cm.*

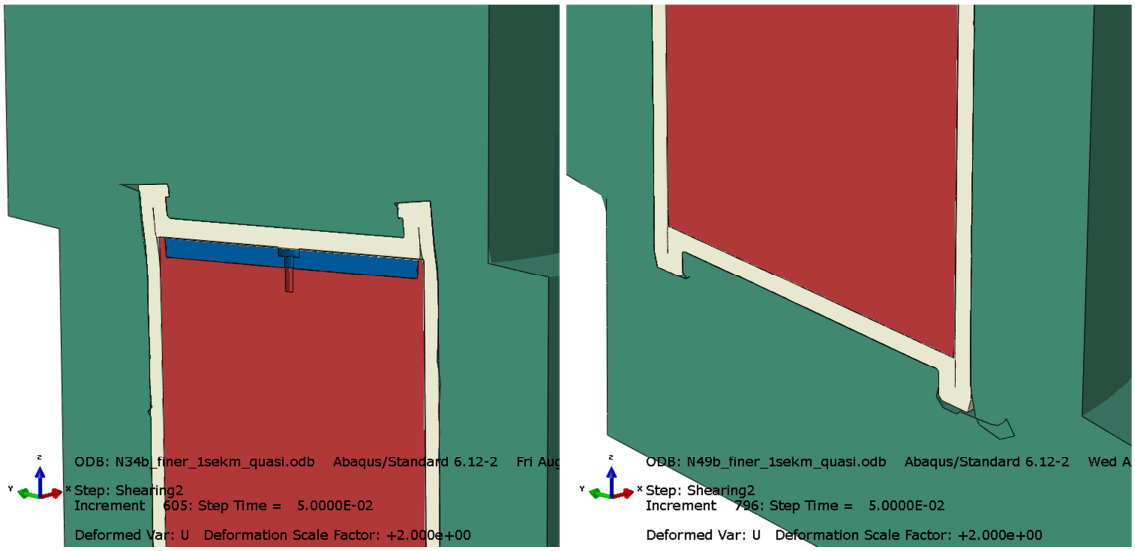

Figure 9-23. *Displaced geometry with scale factor 2 and shearing magnitude 10 cm at the insert lid (left) and at the insert base (right).*

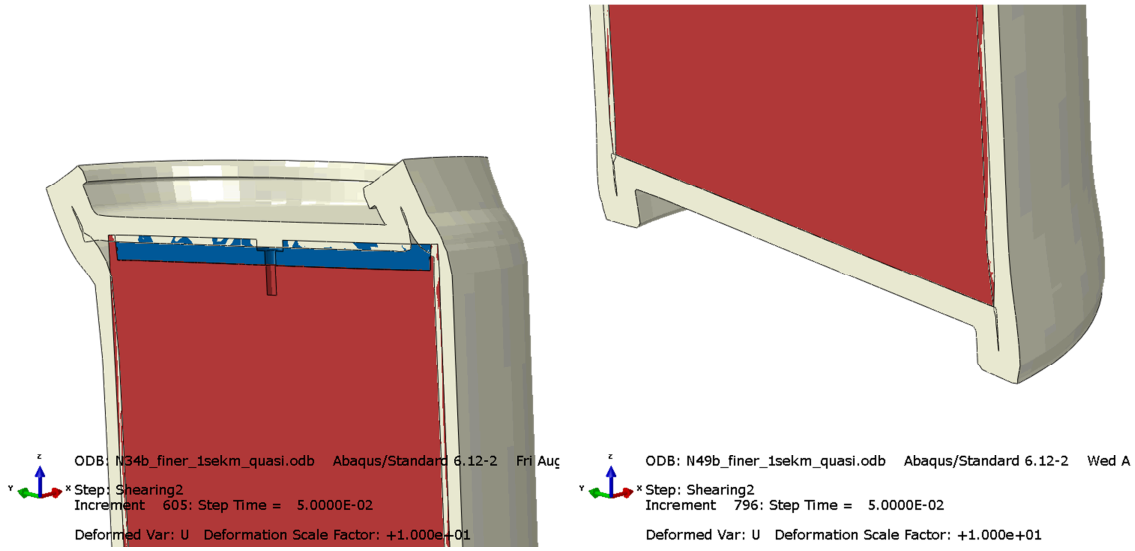

Figure 9-24. *Displaced geometry with scale factor 10 and shearing magnitude 10 cm at the insert lid (left) and at the insert base (right).*

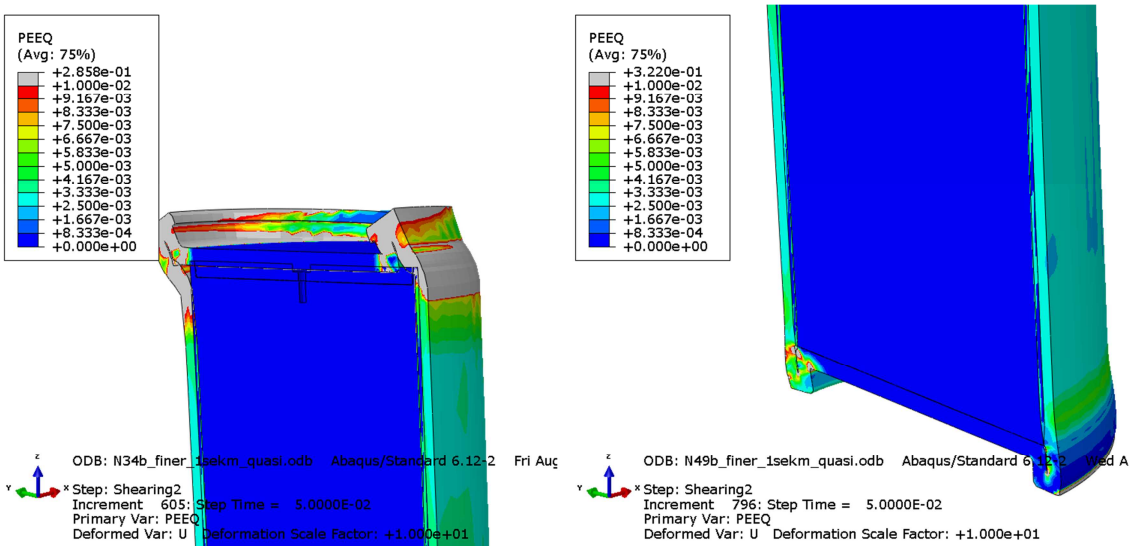

Figure 9-25. *Displaced geometry with scale factor 10 and shearing magnitude 10 cm showing PEEQ (plastic equivalent strain) at the insert lid (left) and at the insert base (right).*

10 Uncertainties

The obtained results are based on several assumptions regarding loads and material properties. Also the discretization in the computer model will affect the results. Some of these influencing factors are addressed below:

- Strain rate effects for bentonite, copper and iron will affect the results. Copper shell will have the strain rate effect included when the strain rate dependency is included.
- All experiments used for material calibration have a spread which will imply a range for the properties defining each material model.
- The yield surface for nodular cast iron is pressure dependent but the performed analyses are based on the Mises material model which is pressure independent which will affect the results. However, material data used in the simulations are based on tensile test data which should be conservative.
- Swelling pressure for the bentonite will affect the material stiffness. The experimental results have a spread in the results and the used data should be conservative in the sense that the obtained stress and strain magnitudes are overestimated.
- Element mesh is rather fine but nevertheless it is too coarse in some regions, especially at the welds and regions with geometric discontinuities. A more refined mesh will probably increase the maximum stress and strain levels. Fortunately, the use of non-linear material properties (such as plasticity and creep) will decrease the sensitivity on the used mesh. The used mesh has been judged to be accurate enough considering also the required computer resources to obtain the results. Since several models have been executed with different mesh densities it has been possible to compare and the conclusion is that the mesh in a global sense is accurate.

11 Evaluation and conclusions

The results obtained from the rock shear analyses could be summarized as:

- The results should vary smoothly with shearing magnitude. However, the obtained results show sometimes a discontinuous variation. This could be explained by the FE-discretization where e.g. the contact conditions sometimes suddenly changes. Another reason is the averaging method when the results are plotted where large gradients could affect the calculated nodal values in non-smooth way.

- The maximum plastic strain in copper shell occurs in fillets (besides regions containing singularities). The maximum plastic strains in the insert occur at the corners of a specific channel. However, the magnitude is small compared to ultimate strains and is considered not to cause any severe damage.

- Maximum principal stress in the insert mainly comes from bending of the shell – the level depends mainly on material properties for the insert (and dimensions) and buffer.

- Material dependency on strain rate has been considered for all cases.

- Shearing at the lid or at the base implies about the same maximum strain levels in the copper shell (about 40% for 10 cm shearing and about 23% for 5 cm shearing) and doesn't seem to cause any severe damage.

References

ABAQUS, 2012. Version 6.1.2. Dassault Systèmes Simulia Corp.

Börgesson L, Hernelind J, 2006. Earthquake induced rock shear through a deposition hole. Influence of shear plane inclination and location as well as buffer properties on the damage caused to the canister. SKB TR-06-43, Svensk Kärnbränslehantering AB.

Börgesson L, Johannesson L-E, Sandén T, Hernelind J, 1995. Modeling of the physical behavior of water saturated clay barriers. Laboratory tests, material models and finite element application. SKB TR 95-20, Svensk Kärnbränslehantering AB.

Börgesson L, Johannesson L-E, Hernelind J, 2004. Earthquake induced rock shear through a deposition hole. Effect on the canister and the buffer. SKB TR-04-02, Svensk Kärnbränslehantering AB.

Börgesson L, Dueck A, Johannesson L-E, 2010. Material model for shear of the buffer – evaluation of laboratory test results. SKB TR-10-31, Svensk Kärnbränslehantering AB.

Börgesson L. and Hernelind J., 2010. Earthquake induced rock shear through a deposition hole. Modelling of three model tests scaled 1:10. Verification of the bentonite material and the calculation technique. SKB TR-10-33.

Hernelind J, 2006. Earthquake induced rock shear through a deposition hole when creep is considered – first model. Effect on the canister and the buffer. SKB R-06-87, Svensk Kärnbränslehantering AB.

Hernelind J, 2010. Modelling and analysis of canister and buffer for earthquake induced rock shear and glacial load. SKB TR-10-34, Svensk Kärnbränslehantering AB.

Jin L-Z, Sandström R, 2008. Creep of copper canisters in power-law breakdown. Computational Materials Science 43, 403–416.

Sandström R, Andersson H C M, 2008. Creep in phosphorus alloyed copper during power-law breakdown. Journal of Nuclear Materials 372, 76–88.

Sandström R, Hallgren J, Burman G, 2009. Stress strain flow curves for Cu-OFP. SKB R-09-14, Svensk Kärnbränslehantering AB.

SSABDirekt, 2008. Steelfacts Domex 355 MC. Available at http://www.ssabdirect.com. [19 September 2008].

SS-EN 10025-2:2004. Varmvalsade konstruktionsstål – Del 2: Tekniska leveransbestämmelser för olegerade stål (Hot rolled products of structural steels - Part 2: Technical delivery conditions for non-alloy structural steels). Stockholm: Swedish Standards Institute.

Unpublished documents

SKBdoc id, version	Title	Issuer, year
1203875 ver 1.0	Ritningsförteckning för kapselkomponenter. (In Swedish.)	SKB, 2009
1336557 ver 2.0	PM Probalistisk analys av skjuvlastfallet. (In Swedish.)	Inspecta Technology AB, 2012
1339902 ver 1.0	Global simulation of copper canister – final deposition	SKB, 2013

Appendix 1 – Plots for N34b_finer_1sekm_quasi

Plots showing deformed geometry as contour plots for all parts at shearing magnitude 5 and 10 cm for case N34b_finer_1sekm_user. The view shows the symmetry plane and all deformations are scaled by a factor of two.

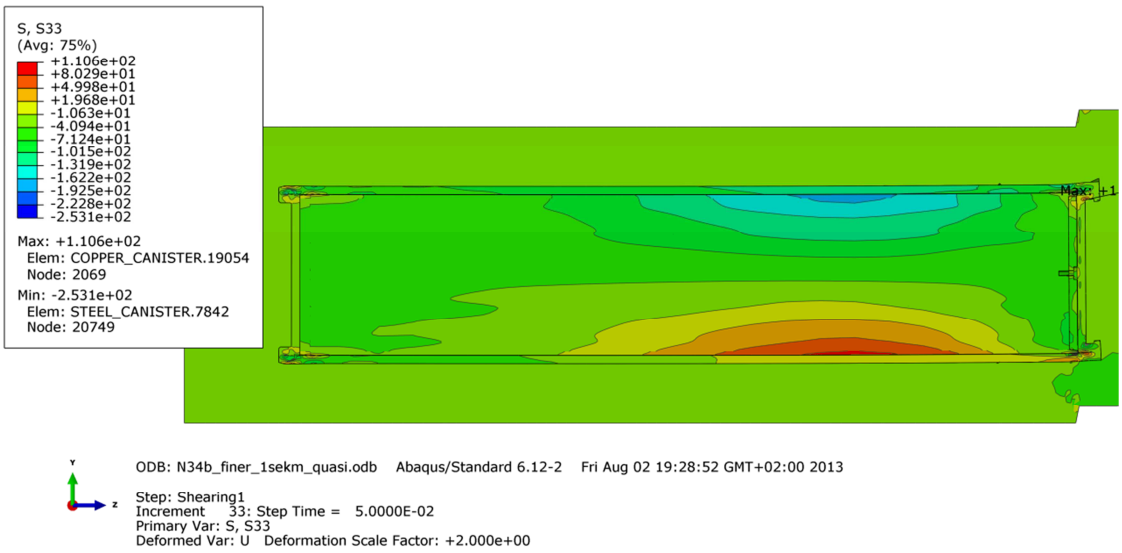

Figure A1-1. *Deformed plot with S33 - 5 cm shearing magnitude.*

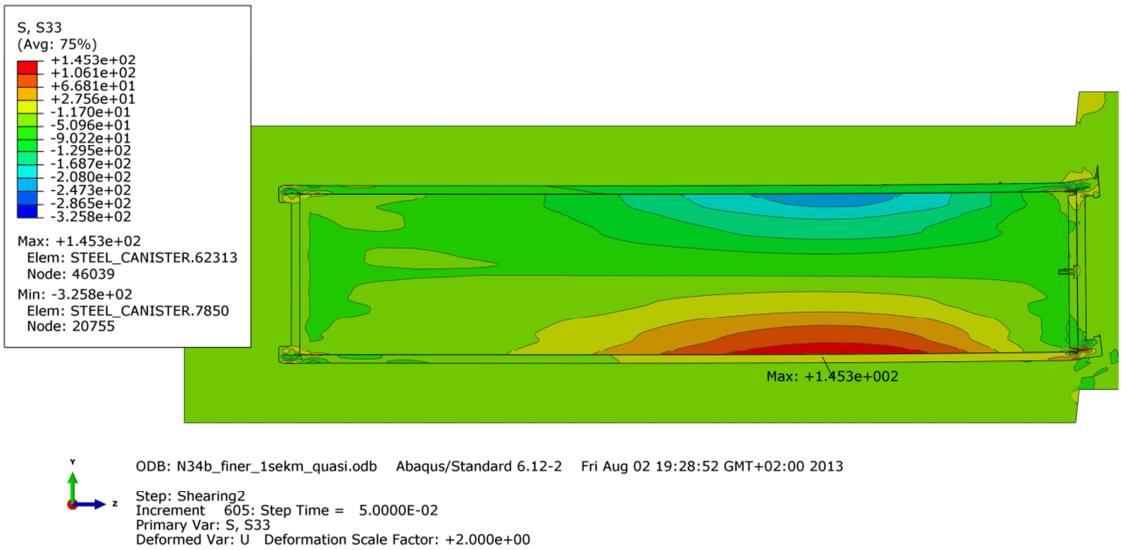

Figure A1-2. Deformed plot with S33 - 10 cm shearing magnitude.

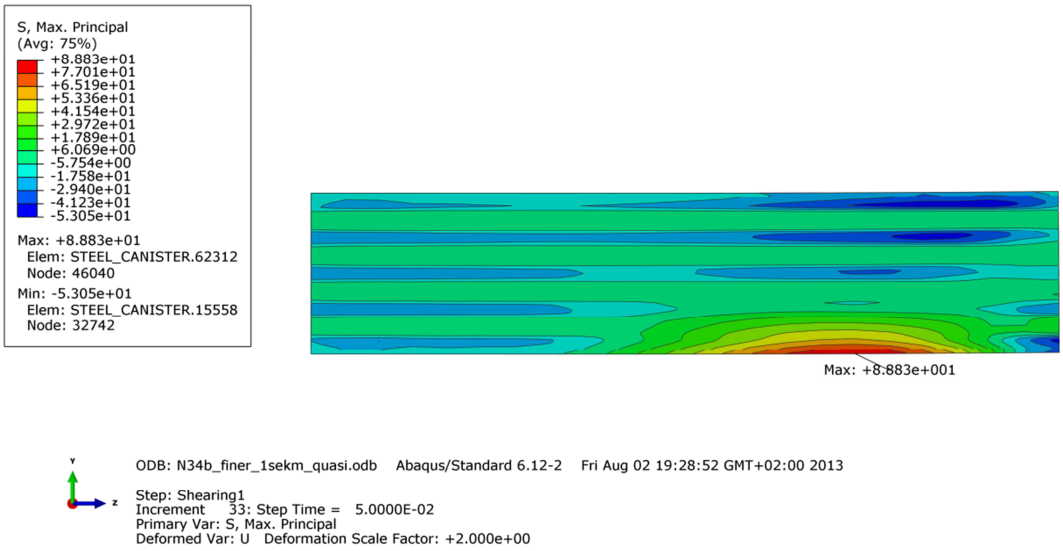

Figure A1-3. Deformed plot with max principal stress for insert- 5 cm shearing magnitude.

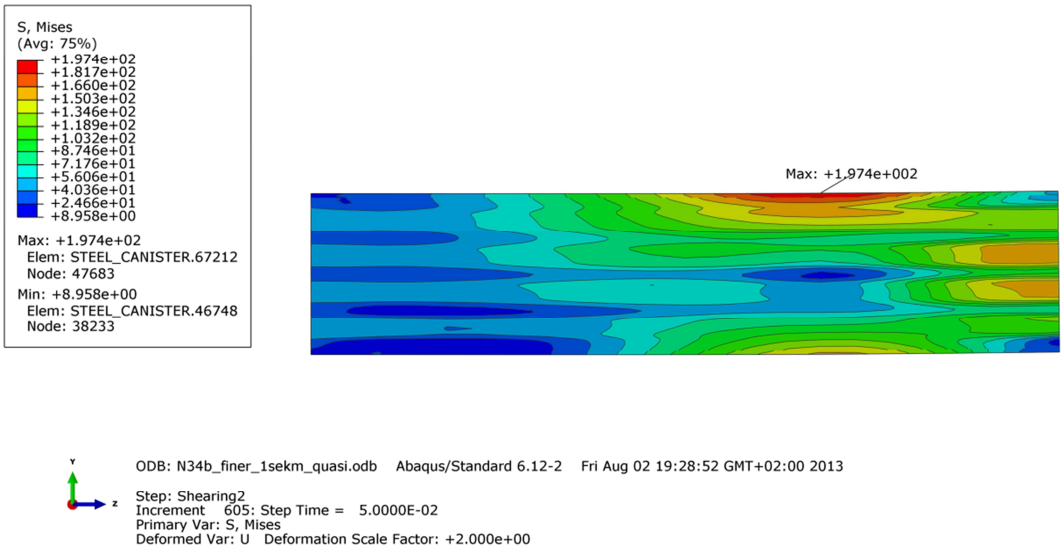

Figure A1-4. Deformed plot with max principal stress for insert - 10 cm shearing magnitude.

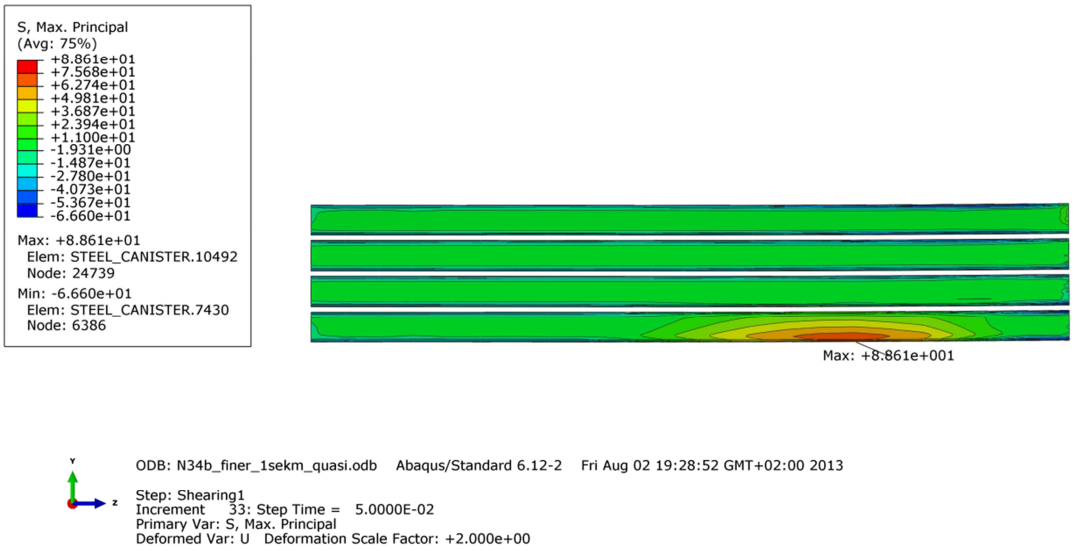

Figure A1-5. Deformed plot with max principal stress for channels - 5 cm shearing magnitude.

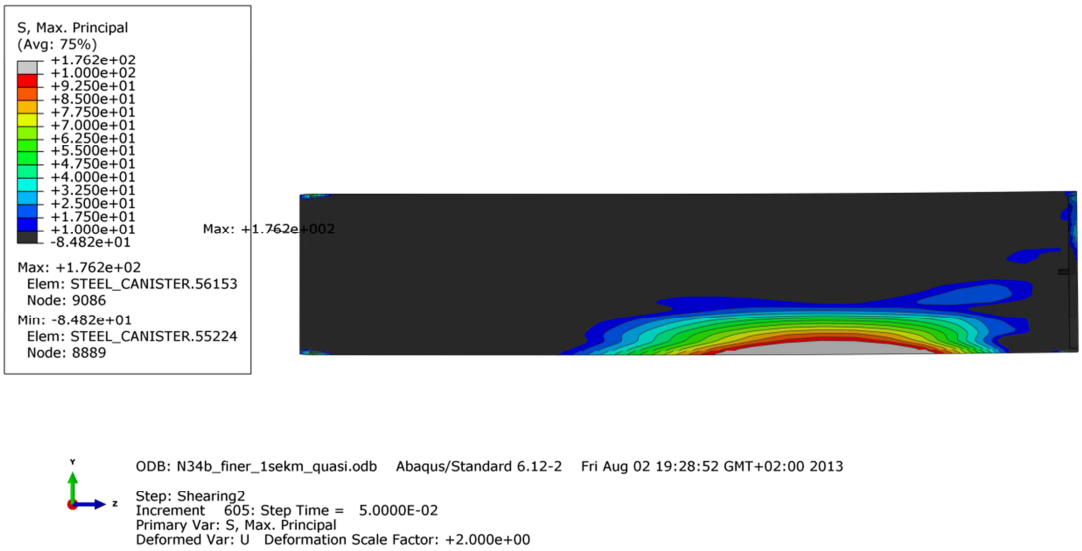

Figure A1-6. Deformed plot with max principal stress for channels - 10 cm shearing magnitude.

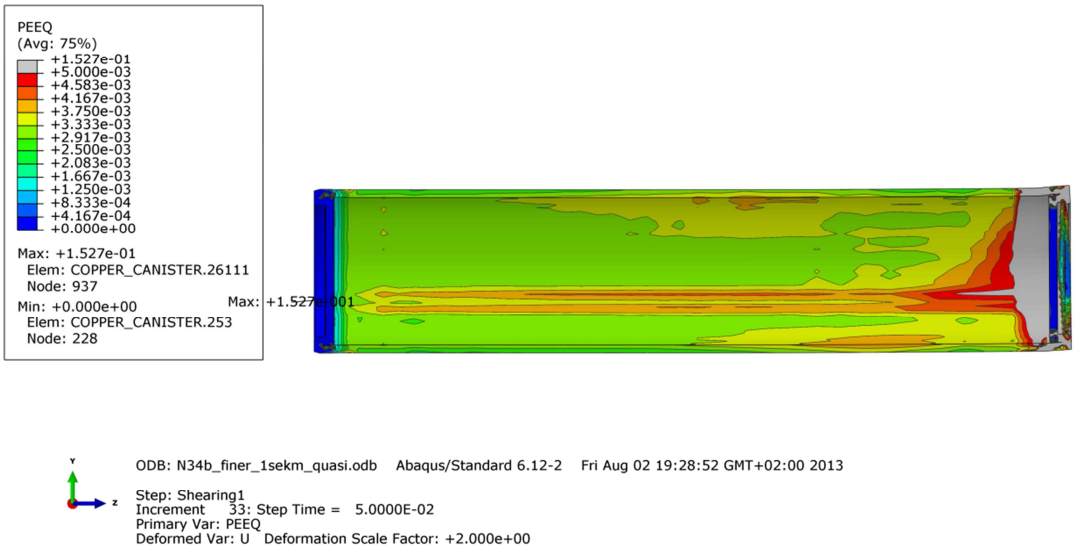

Figure A1-7. *Deformed plot with plastic strain for copper shell - 5 cm shearing magnitude.*

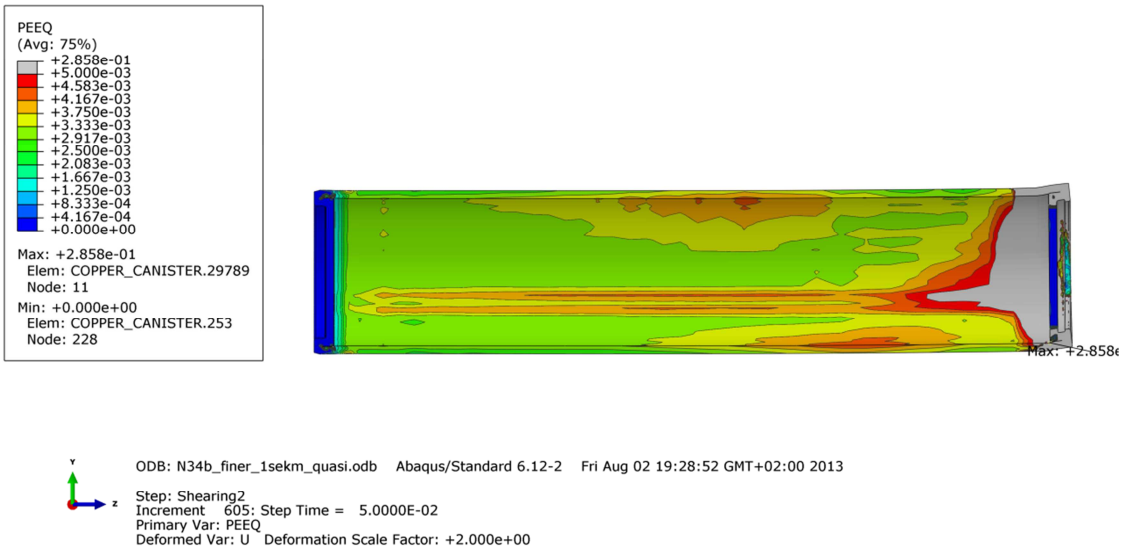

Figure A2-8. *Deformed plot with plastic strain for copper shell - 10 cm shearing magnitude.*

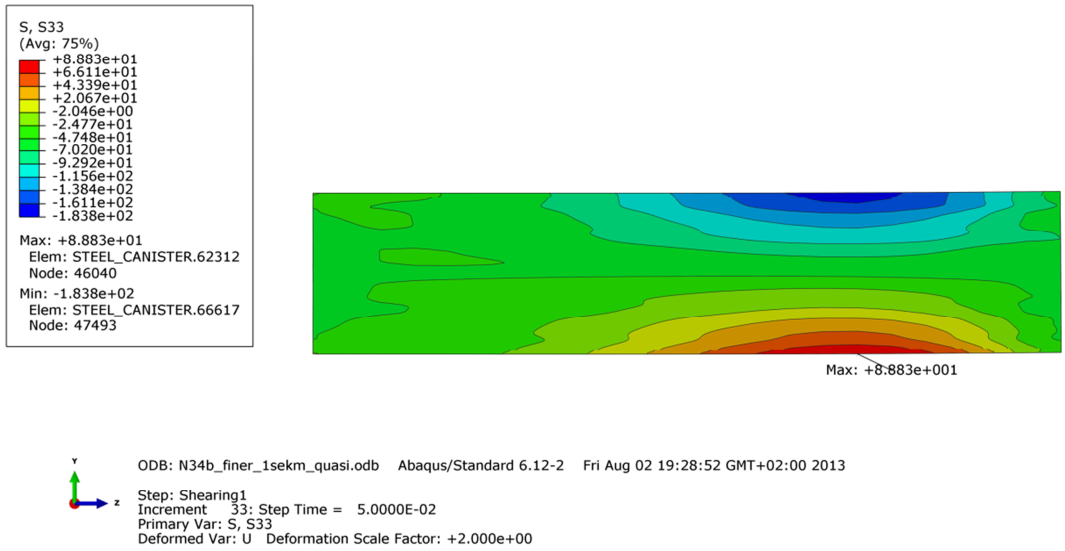

***Figure A1-9**. Deformed plot with axial stress for cast iron insert - 5 cm shearing magnitude.*

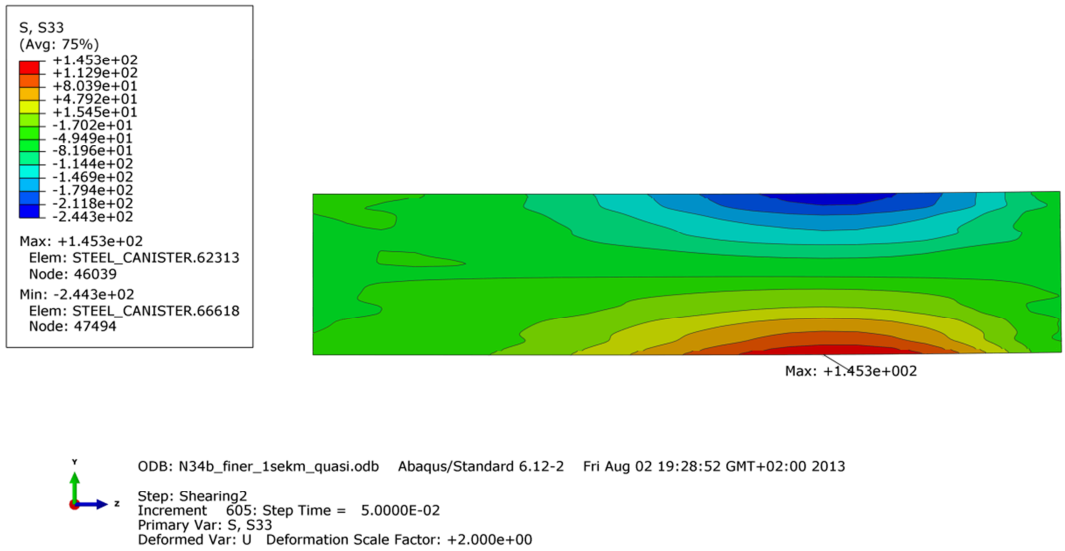

***Figure A1-10.** Deformed plot with axial stress for cast iron insert - 10 cm shearing magnitude.*

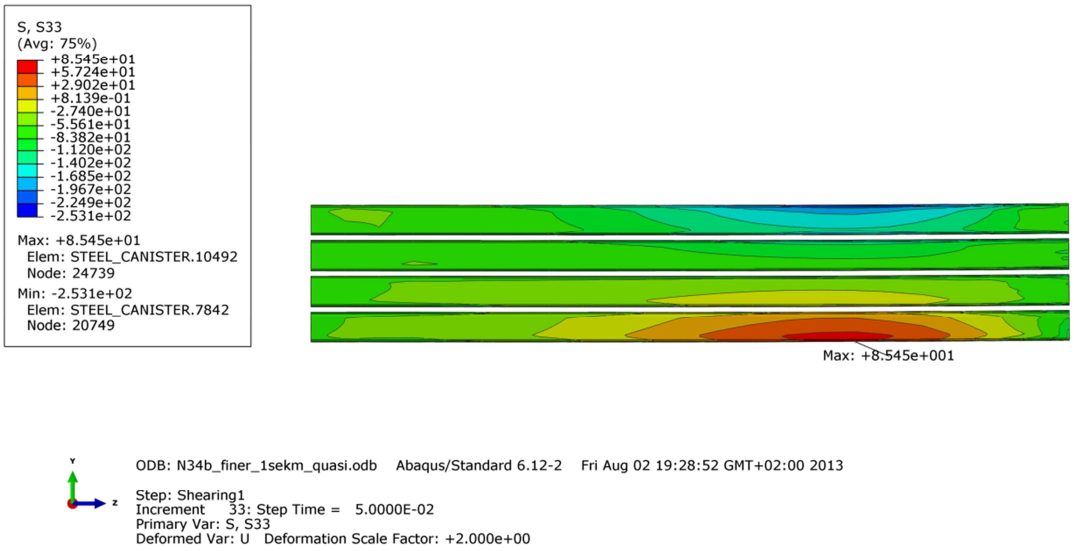

Figure A1-11. *Deformed plot with axial stress for steel channels - 5 cm shearing magnitude.*

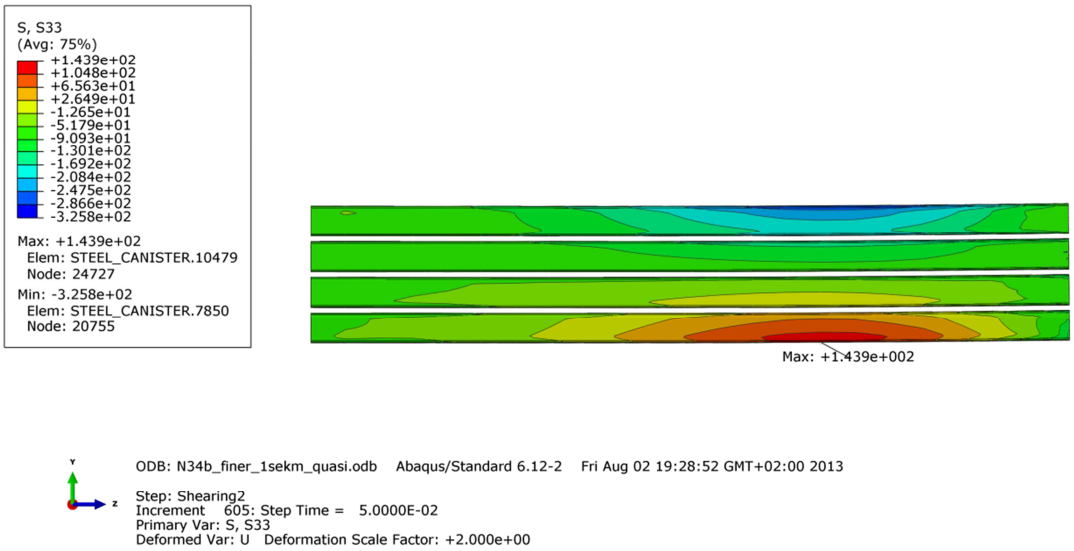

Figure A1-12. *Deformed plot with axial stress for steel channels - 10 cm shearing magnitude.*

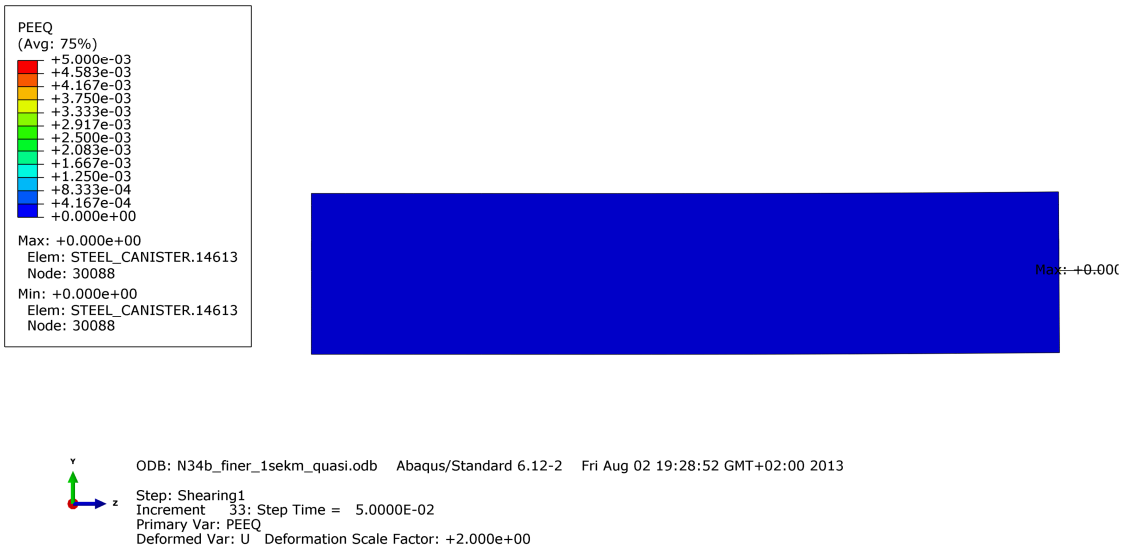

Figure A1-13. *Deformed plot with plastic strain for cast iron insert - 5 cm shearing magnitude.*

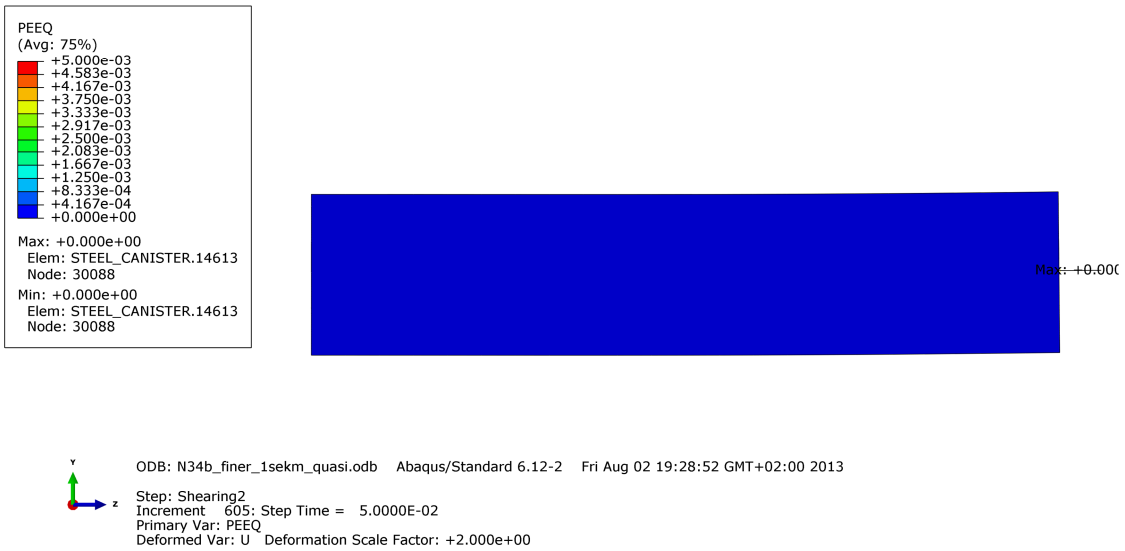

Figure A1-14. *Deformed plot with plastic strain for cast iron insert - 10 cm shearing magnitude.*

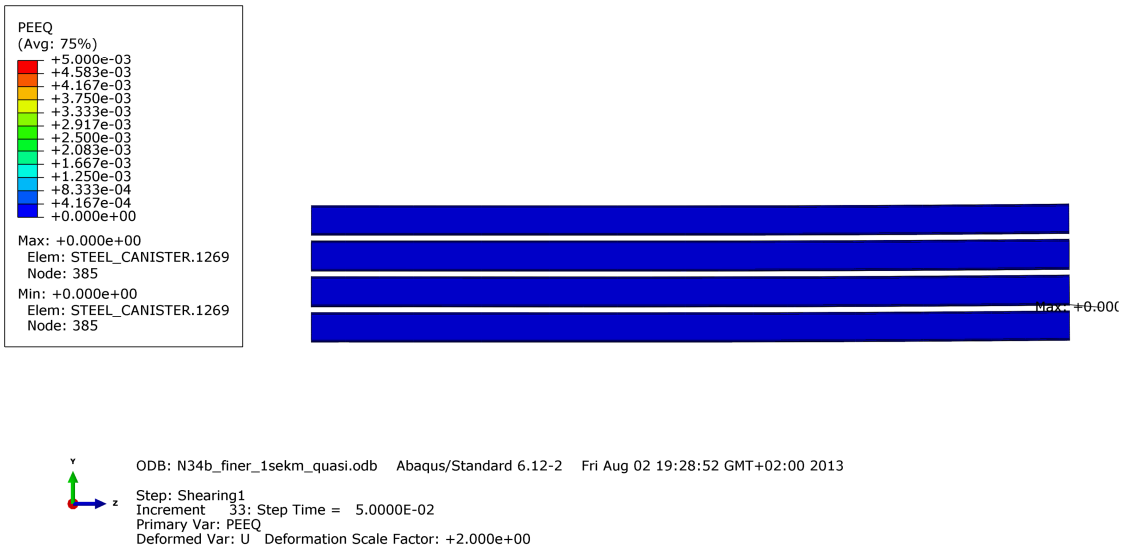

Figure A1-15. *Deformed plot with plastic strain for steel channels - 5 cm shearing magnitude.*

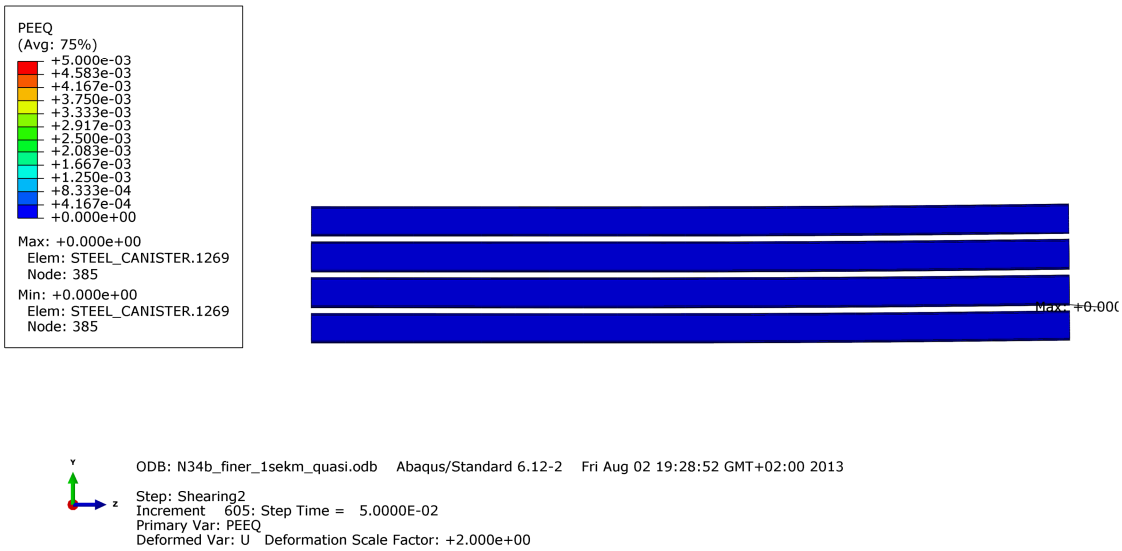

Figure A1-16. *Deformed plot with plastic strain for steel channels - 10 cm shearing magnitude.*

Appendix 2 – Plots for N49b_finer_1sekm_quasi

Plots showing deformed geometry as contour plots for all parts at shearing magnitude 5 and 10 cm for case N49b_finer_1sekm_user. The view shows the symmetry plane and all deformations are scaled by a factor of two.

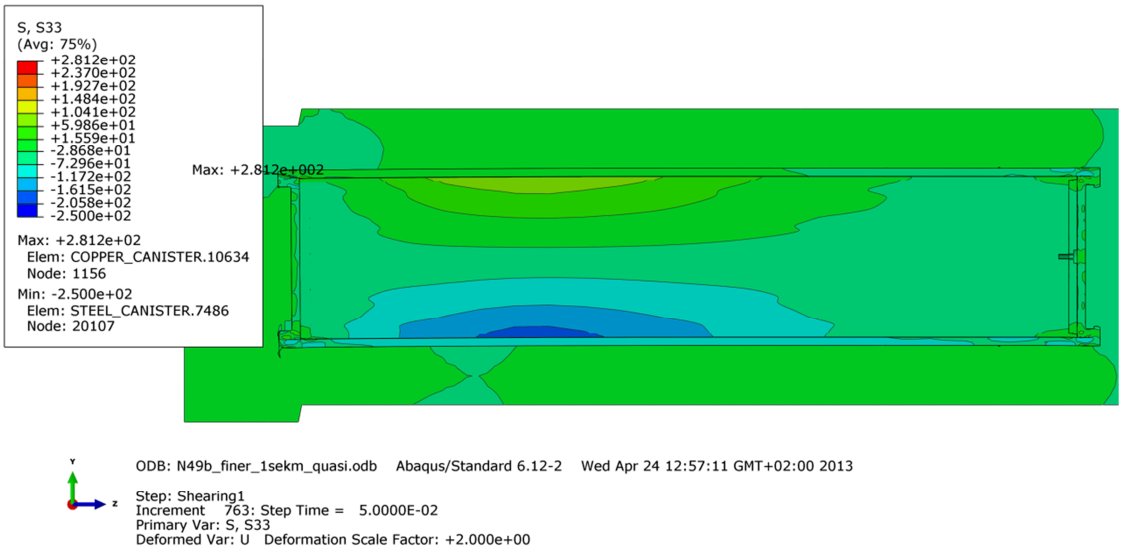

Figure A2-1. *Deformed plot with S33 - 5 cm shearing magnitude.*

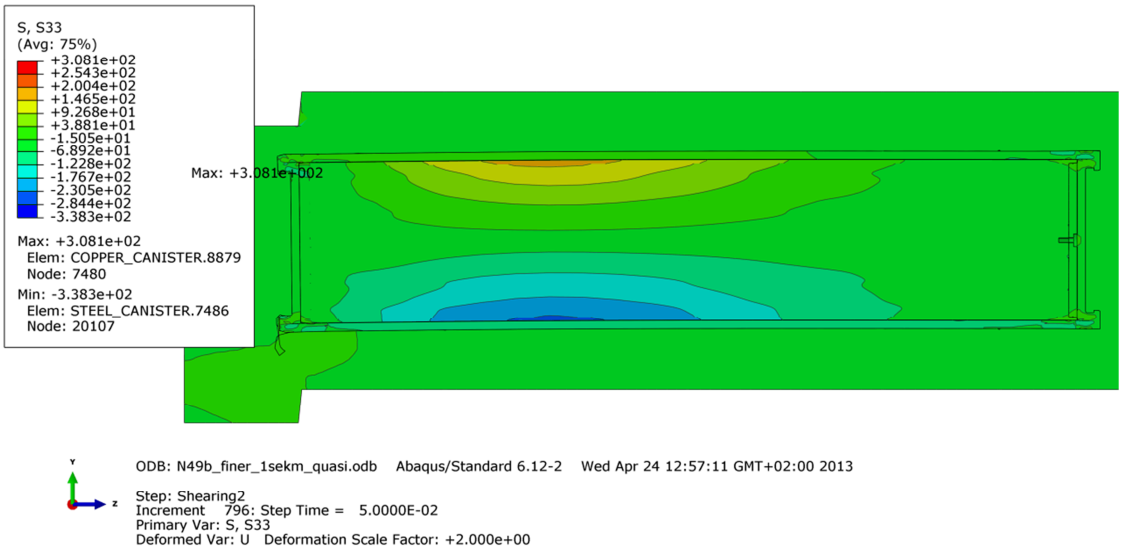

Figure A2-2. *Deformed plot with S33 - 10 cm shearing magnitude.*

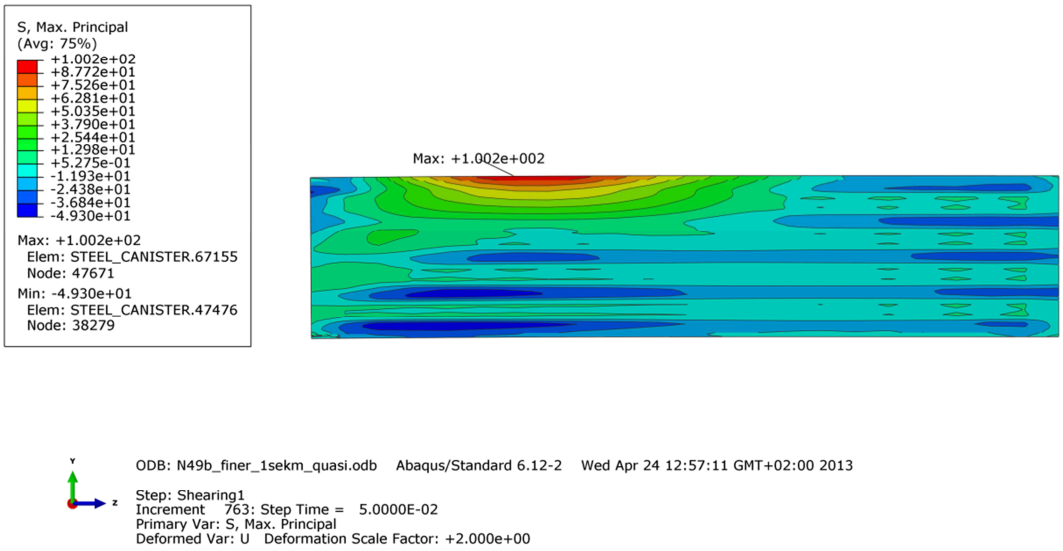

Figure A2-3. *Deformed plot with max principal stress for insert- 5 cm shearing magnitude.*

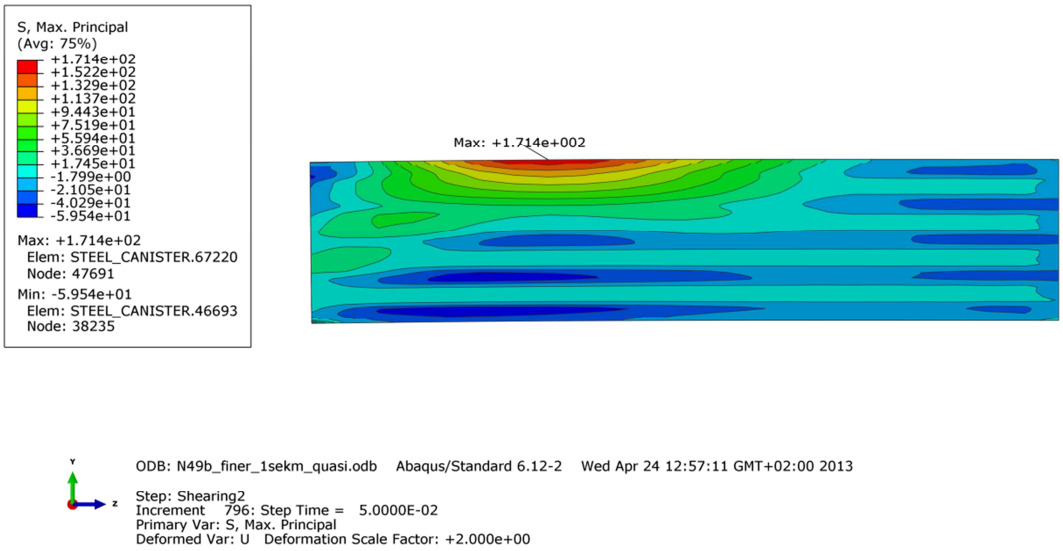

Figure A2-4. *Deformed plot with max principal stress for insert - 10 cm shearing magnitude.*

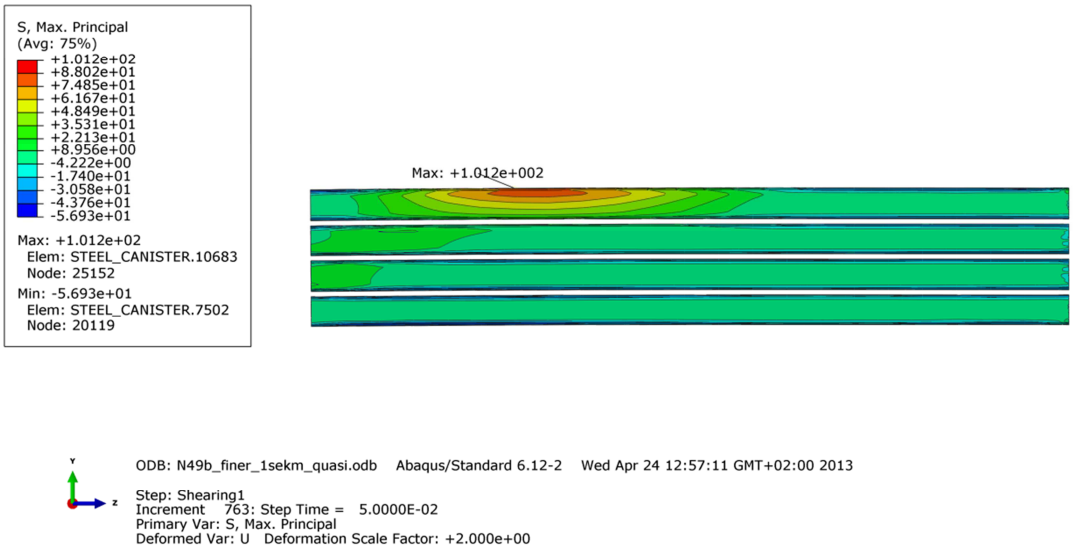

Figure A2-5. *Deformed plot with max principal stress for channels - 5 cm shearing magnitude.*

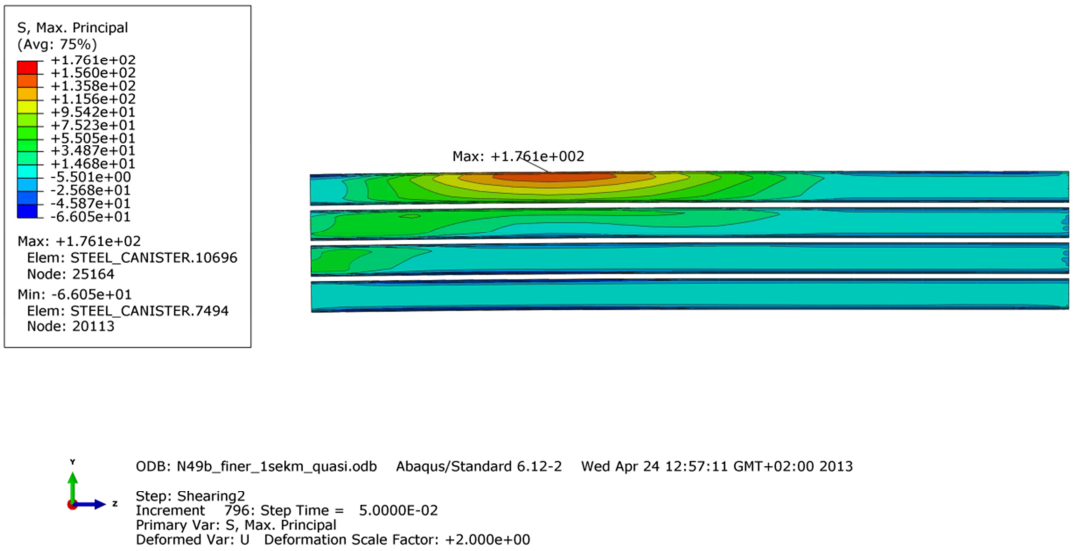

Figure A2-6. *Deformed plot with max principal stress for channels - 10 cm shearing magnitude.*

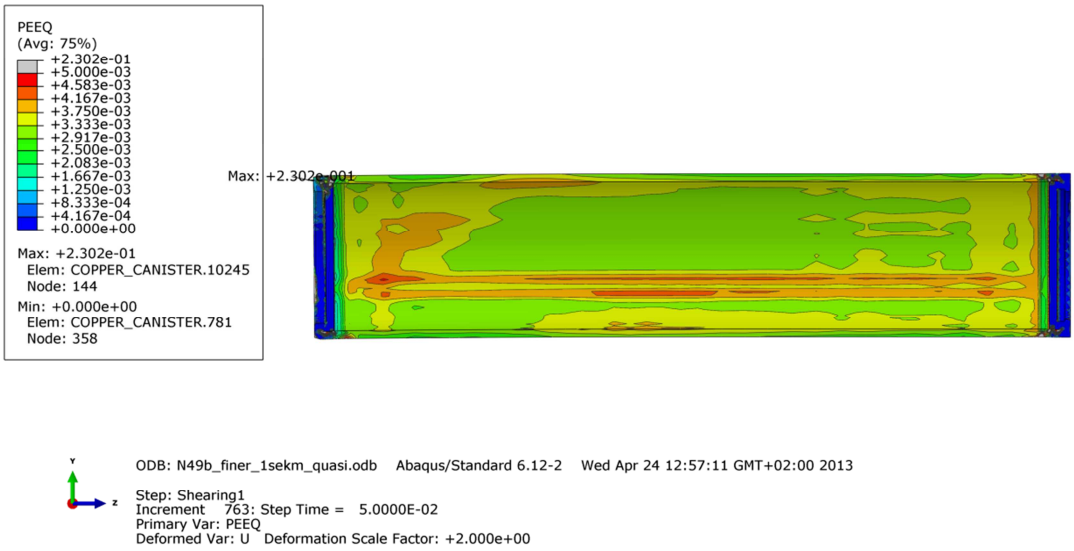

Figure A2-7. *Deformed plot with plastic strain for copper shell - 5 cm shearing magnitude.*

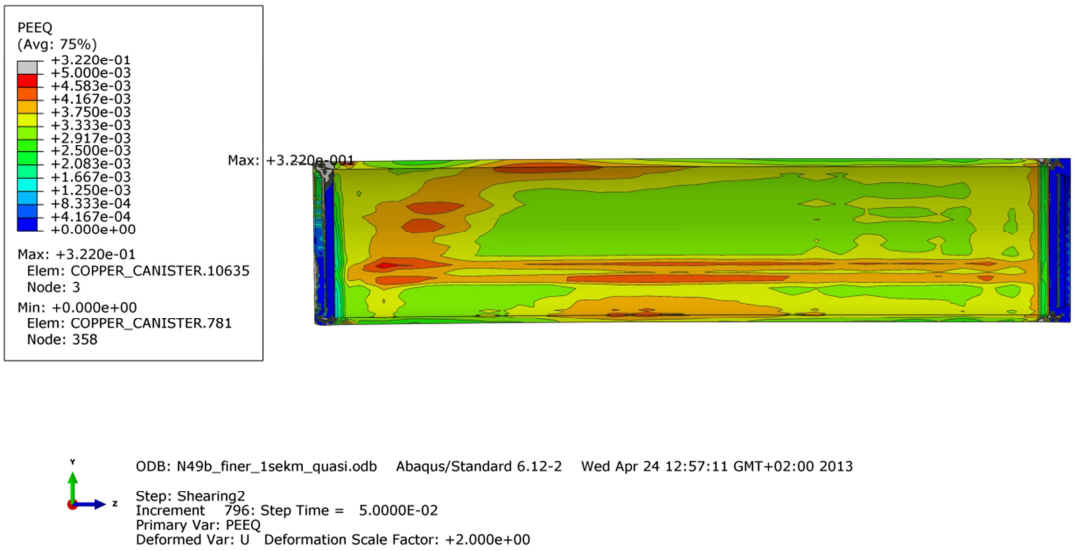

Figure A2-8. *Deformed plot with plastic strain for copper shell - 10 cm shearing magnitude.*

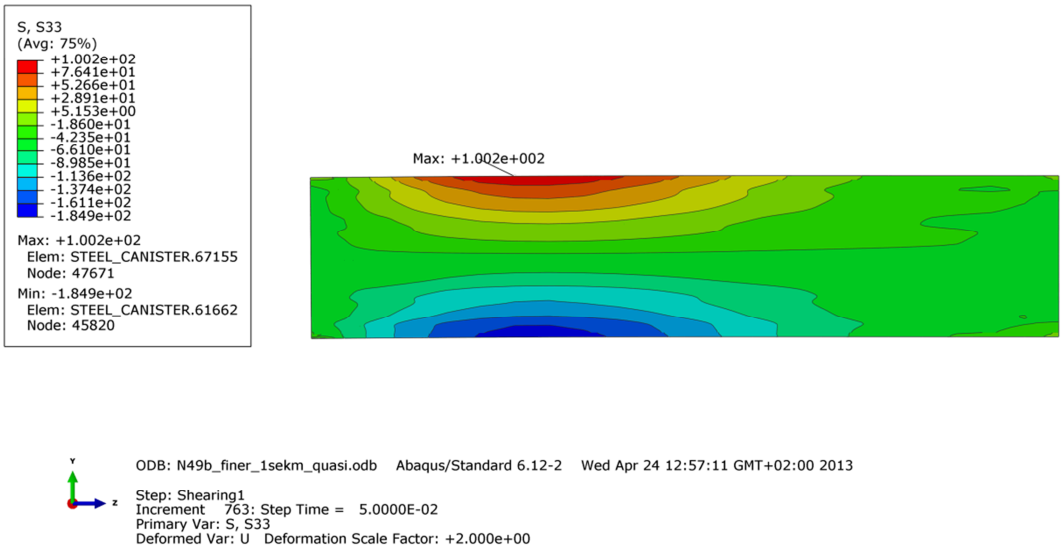

***Figure A2-9**. Deformed plot with axial stress for cast iron insert - 5 cm shearing magnitude.*

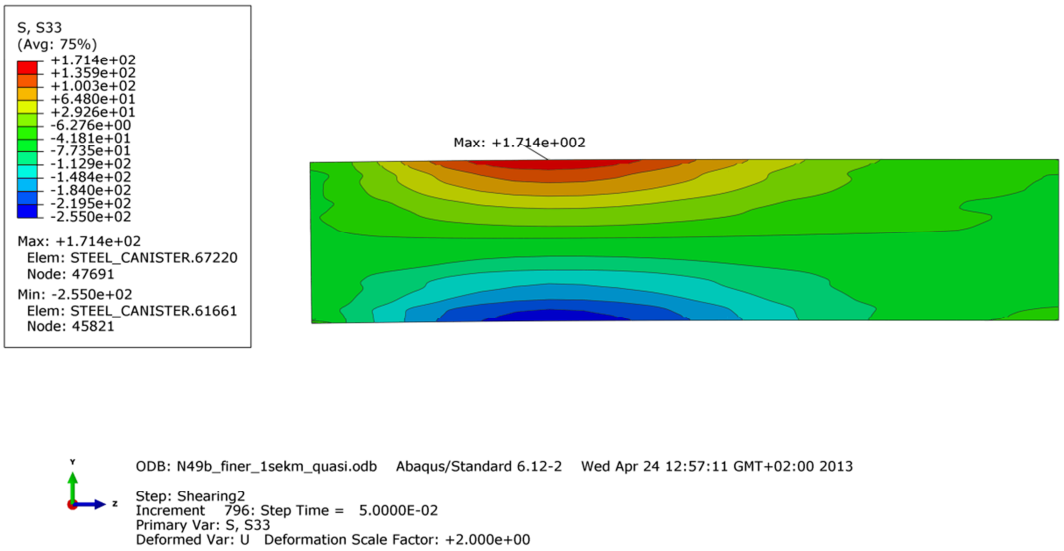

***Figure A2-10.** Deformed plot with axial stress for cast iron insert - 10 cm shearing magnitude.*

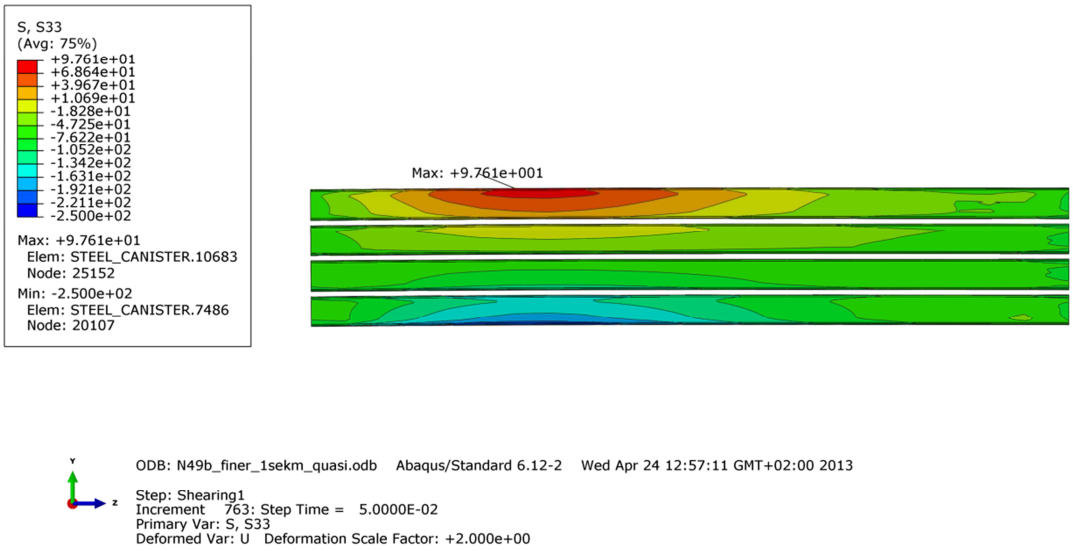

Figure A2-11. *Deformed plot with axial stress for steel channels - 5 cm shearing magnitude.*

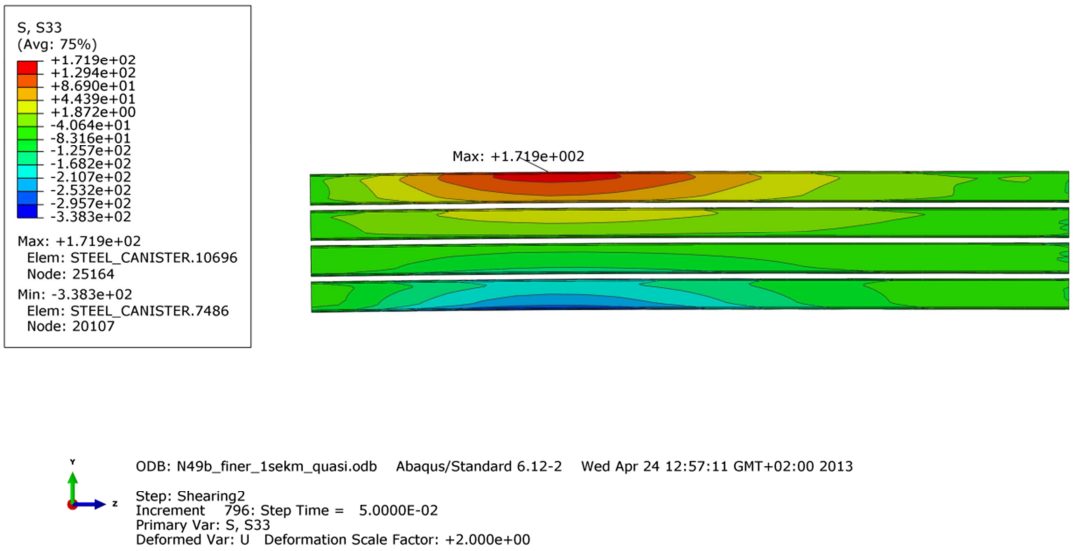

Figure A2-12. *Deformed plot with axial stress for steel channels - 10 cm shearing magnitude.*

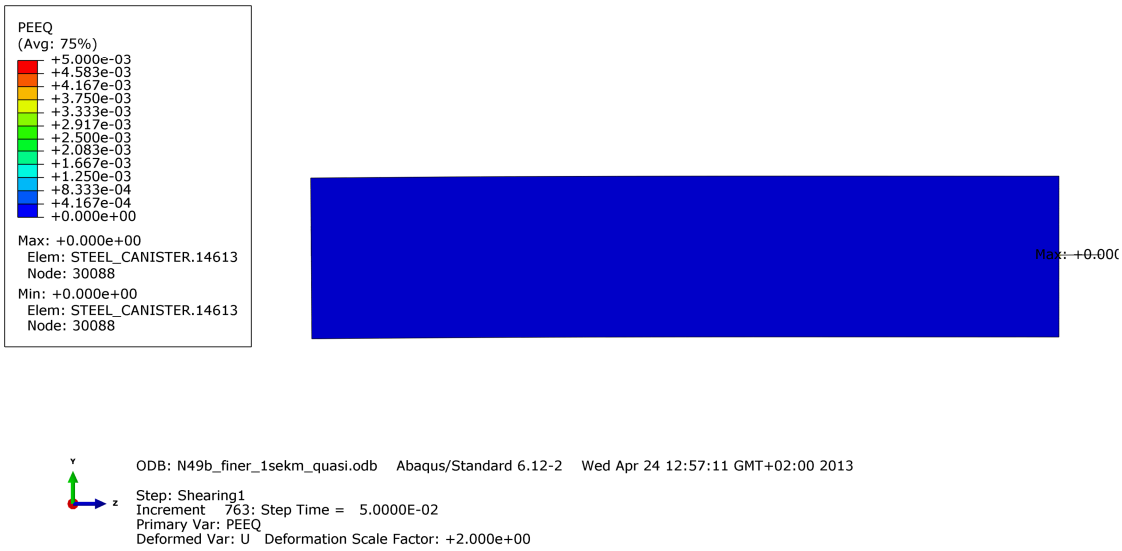

Figure A2-13. *Deformed plot with plastic strain for cast iron insert - 5 cm shearing magnitude.*

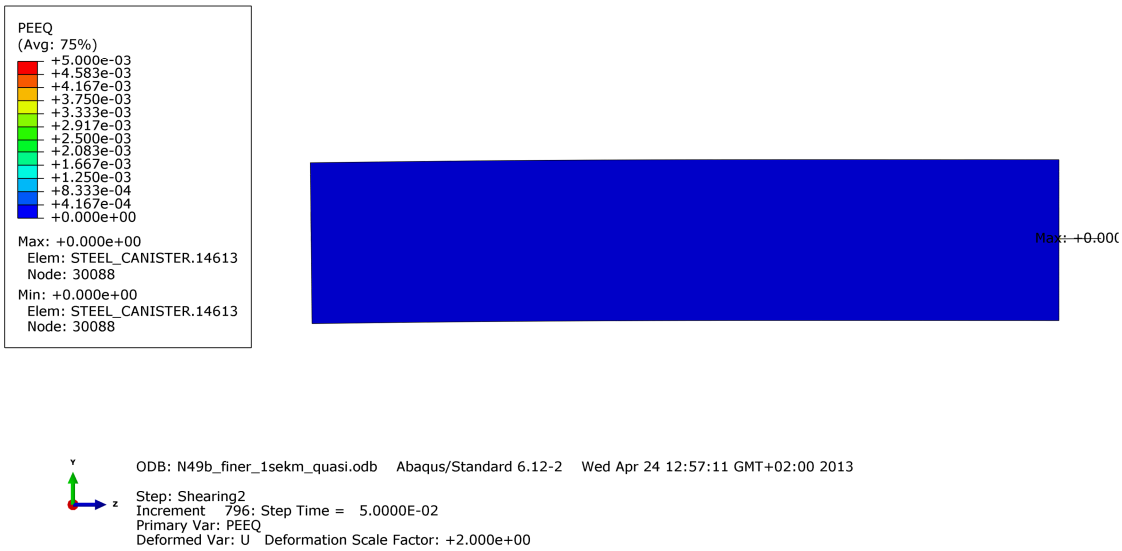

Figure A2-14. *Deformed plot with plastic strain for cast iron insert - 10 cm shearing magnitude.*

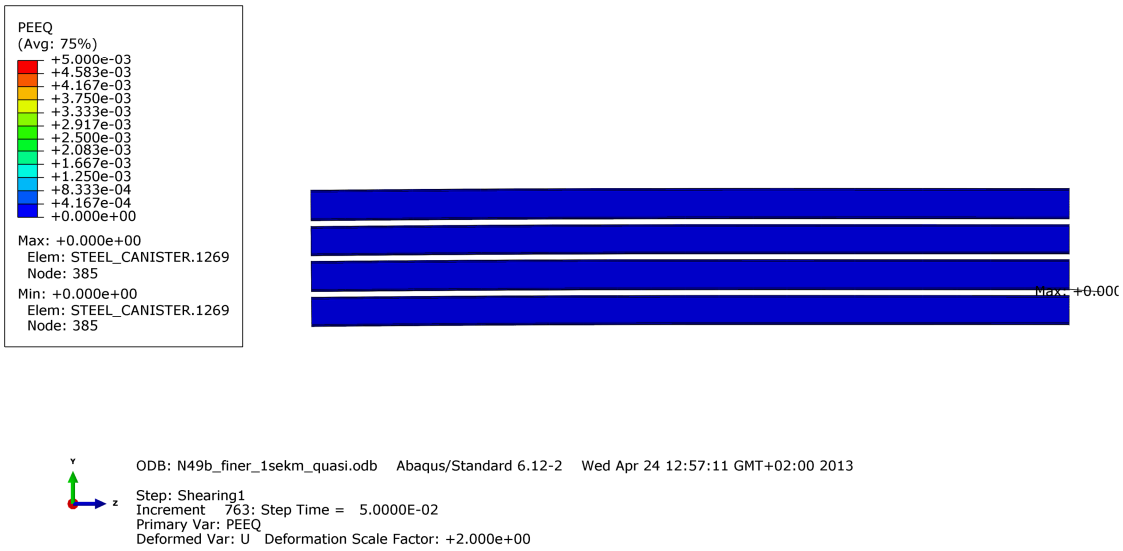

Figure A2-15. *Deformed plot with plastic strain for steel channels - 5 cm shearing magnitude.*

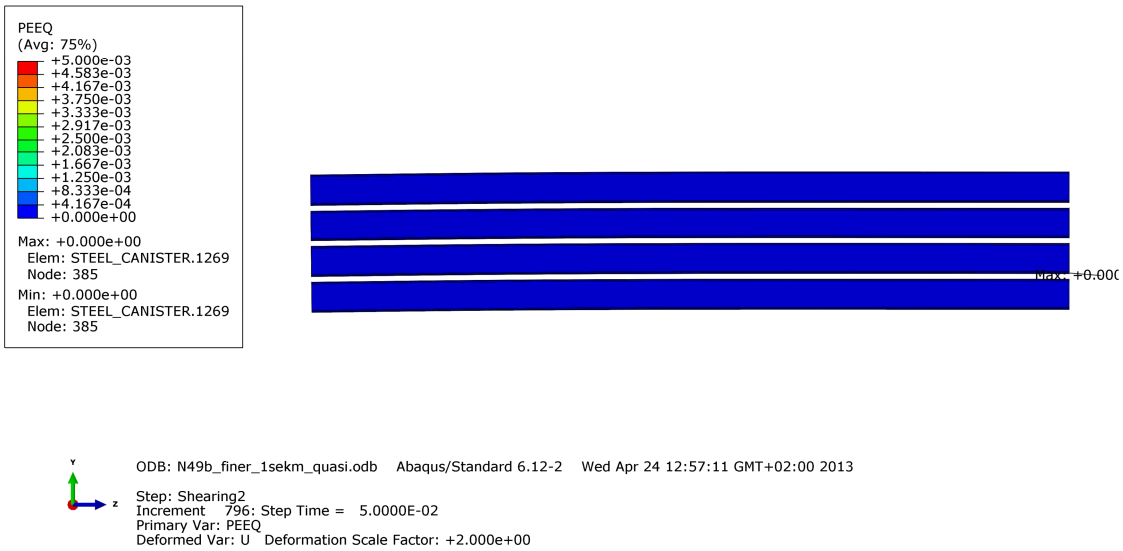

Figure A2-16. *Deformed plot with plastic strain for steel channels - 10 cm shearing magnitude.*

Appendix 3 – Storage of files

This report is based on the results from a lot of FE-simulations using ABAQUS which is a commercial available code and is thus not stored as part of the work. Below is a short description of files used in the project and directories for storage of these. These files are also stored at SKB.

The files are stored in directories as:

Geometry Input-files Plots lid_base_shearing.docx - this report Scripts

1 – Plot-files used in the report

Contents in C:\Users\jhd\mappar\skb\ssm_questions\bottom_top\Plots

n49b_partions.png
n34_49-3d_peeq_copper.png
n34_49_3d_deformed_end2.png
n34_49_3d_deformed_end.png
N49b_finer_1sekm_quasi-3d_deformed.png
N34b_finer_1sekm_quasi-3d_deformed.png
only_N49b_finer_1sekm-5cm-copper_peeq.png
only_N49b_finer_1sekm-5cm-copper_peeq_corner1.png
only_N49b_finer_1sekm-5cm-copper_peeq_corner2.png
only_N49b_finer_1sekm-5cm-copper_mises_corner2.png
only_N49b_finer_1sekm-5cm-copper_mises_corner1.png
only_N49b_finer_1sekm-5cm-copper_mises.png
only_N49b_finer_1sekm-5cm-insert_peeq.png
only_N49b_finer_1sekm-5cm-insert_mises.png
only_N49b_finer_1sekm-5cm-peeq.png
only_N34b_finer_1sekm-5cm-copper_peeq_corner2.png
only_N34b_finer_1sekm-5cm-copper_mises_corner2.png
only_N34b_finer_1sekm-5cm-copper_mises.png
only_N34b_finer_1sekm-5cm-copper_mises_corner1.png
only_N34b_finer_1sekm-5cm-copper_peeq_corner1.png
only_N34b_finer_1sekm-5cm-copper_peeq.png
only_N34b_finer_1sekm-5cm-insert_peeq.png
only_N34b_finer_1sekm-5cm-insert_mises2.png
only_N34b_finer_1sekm-5cm-insert_mises.png
only_N34b_finer_1sekm-5cm-peeq.png
only_N49b_finer_1sekm-10cm-copper_peeq.png
only_N49b_finer_1sekm-10cm-copper_peeq_corner1.png
only_N49b_finer_1sekm-10cm-copper_peeq_corner2.png
only_N49b_finer_1sekm-10cm-copper_mises_corner2.png
only_N49b_finer_1sekm-10cm-copper_mises_corner1.png
only_N49b_finer_1sekm-10cm-copper_mises.png
only_N49b_finer_1sekm-10cm-insert_peeq.png
only_N49b_finer_1sekm-10cm-insert_mises.png
only_N49b_finer_1sekm-10cm-peeq.png
only_N34b_finer_1sekm-10cm-copper_peeq_corner2.png
only_N34b_finer_1sekm-10cm-copper_mises_corner2.png
only_N34b_finer_1sekm-10cm-copper_mises.png
only_N34b_finer_1sekm-10cm-copper_mises_corner1.png
only_N34b_finer_1sekm-10cm-copper_peeq_corner1.png
only_N34b_finer_1sekm-10cm-copper_peeq.png
only_N34b_finer_1sekm-10cm-insert_peeq.png
only_N34b_finer_1sekm-10cm-insert_mises2.png
only_N34b_finer_1sekm-10cm-insert_mises.png
only_N34b_finer_1sekm-10cm-peeq.png

Plot files used in the report

Appendix 1
N34b_finer_1sekm_quasi 10cm S33 insert_channels.png
N34b_finer_1sekm_quasi 10cm maxPrin insert_channels.png
N34b_finer_1sekm_quasi 10cm peeq insert_channels.png
N34b_finer_1sekm_quasi 10cm mises insert_channels.png
N34b_finer_1sekm_quasi 10cm peeq insert_nochannels.png
N34b_finer_1sekm_quasi 10cm maxPrin insert_nochannels.png
N34b_finer_1sekm_quasi 10cm S33 insert_nochannels.png
N34b_finer_1sekm_quasi 10cm mises insert_nochannels.png
N34b_finer_1sekm_quasi 10cm peeq insert.png
N34b_finer_1sekm_quasi 10cm maxPrin insert.png
N34b_finer_1sekm_quasi 10cm S33 insert.png
N34b_finer_1sekm_quasi 10cm mises insert.png
N34b_finer_1sekm_quasi 10cm mises copper.png
N34b_finer_1sekm_quasi 10cm peeq copper.png
N34b_finer_1sekm_quasi 10cm peeq.png
N34b_finer_1sekm_quasi 10cm deformed.png

Appendix 2
N49b_finer_1sekm_quasi 10cm S33 insert_channels.png
N49b_finer_1sekm_quasi 10cm maxPrin insert_channels.png
N49b_finer_1sekm_quasi 10cm peeq insert_channels.png
N49b_finer_1sekm_quasi 10cm mises insert_channels.png
N49b_finer_1sekm_quasi 10cm peeq insert_nochannels.png
N49b_finer_1sekm_quasi 10cm maxPrin insert_nochannels.png
N49b_finer_1sekm_quasi 10cm S33 insert_nochannels.png
N49b_finer_1sekm_quasi 10cm mises insert_nochannels.png
N49b_finer_1sekm_quasi 10cm peeq insert.png
N49b_finer_1sekm_quasi 10cm maxPrin insert.png
N49b_finer_1sekm_quasi 10cm S33 insert.png
N49b_finer_1sekm_quasi 10cm mises insert.png
N49b_finer_1sekm_quasi 10cm mises copper.png
N49b_finer_1sekm_quasi 10cm peeq copper.png
N49b_finer_1sekm_quasi 10cm peeq.png
N49b_finer_1sekm_quasi 10cm deformed.png

2 – Input files used for the simulations

Each analysis is started by abaqus job=input-file (w/o .inp).

Files with extension “incl” are referenced by some of the input-files (extension “inp”).

Contents in C:\Users\jhd\mappar\skb\ssm_questions\bottom_top\Input-files

N49b_finer_1sekm_quasi.inp	- shearing at base with global model
N34b_finer_1sekm_quasi.inp	- shearing at lid with global model
assembly_finer_10.incl	- include file
assembly_finer_10_quasi.incl	- include file
assembly2_finer_user.incl	- include file
insert_lid.incl	- include file
insert_finer.incl	- include file
insert_canister.incl	- include file
bentonite.incl	- include file
bentonite_10.incl	- include file
copper_canister.incl	- include file
material_copper.incl	- include file

4 – Scripts used for post-processing

Used inside ABAQUS/CAE or by abaqus cae startup=script.py after appropriate editing of job-name inside the script-file.

Contents in C:\Users\jhd\mappar\skb\ssm_questions\bottom_top\\Scripts

contour2_plots.py - script for contour plots of Global analysis
only_n34b_finer_1sekm.py - script for comparing results of Global analyses
n34_49-3d_deformed.py - script for 3d-plots

5 – Geometry definitions

Contents in C:\Users\jhd\mappar\skb\ssm_questions\bottom_top\Geometry

global_parameters.cae - ABAQUS/CAE-database
global_parameters.jnl - ABAQUS/CAE-journal file